arXiv:1604.05739v2 [gr-qc] 21 Jun 2016

High-order Primordial Perturbations with Quantum Gravitational Effects

Tao Zhu[a,b,*] Anzhong Wang[a,b,c,†] Klaus Kirsten[d,‡] Gerald Cleaver[e,§] and Qin Sheng[d¶]
[a] *Institute for Advanced Physics & Mathematics, Zhejiang University of Technology, Hangzhou, 310032, China*
[b] *GCAP-CASPER, Physics Department, Baylor University, Waco, TX 76798-7316, USA*
[c] *Departamento de Física Teórica, Instituto de Física, UERJ, 20550-900, Rio de Janeiro, Brazil*
[d] *GCAP-CASPER, Mathematics Department, Baylor University, Waco, TX 76798-7328, USA*
[e] *EUCOS-CASPER, Physics Department, Baylor University, Waco, TX 76798-7316, USA*
(Dated: June 22, 2016)

In this paper, we provide a systematic investigation of high-order primordial perturbations with nonlinear dispersion relations due to quantum gravitational effects in the framework of *uniform asymptotic approximations*. Because of these effects, the equation of motion of the mode function in general has multiple-turning points. After obtaining analytically approximated solutions to any order in different regions, associated with different types of turning points, we match them to the third one. To this order the errors are less than 0.15%. General expressions of the power spectra of the primordial tensor and scalar perturbations are derived explicitly. We also investigate effects of back-reactions of the quantum gravitational corrections, and make sure that inflation lasts long enough in order to solve the underlying problems, such as flatness, horizon and monopole. Then, we study various features of the spectra that are observationally relevant. In particular, under a moderate assumption about the energy scale of the underlying theory of quantum gravity, we have shown that the quantum gravitational effects may alter significantly the ratio between the tensor and scalar power spectra, thereby providing a natural mechanism to alleviate the tension between observations and certain inflationary models, including the one with a quadratic potential.

I. INTRODUCTION

The paradigm of cosmic inflation has had remarkable success in solving many problems elegantly with standard big bang cosmology and predicting the primordial power spectrum whose evolution explains both the formation of the large scale structure of the universe and the small inhomogeneities in the cosmic microwave background (CMB) [1]. These are now matched to observations with a spectacular precision [2–4]. However, as it is well known, the inflationary scenario is conceptually incomplete in several respects. For example, in some inflation models, the energy scale of quantum fluctuations, which relates to the present observations, was not far from the Planck energy in the beginning of the inflation [5, 6]. This leads to the problem that the underlying quantum field theory on classical spacetime becomes unreliable. In addition, the evolution of the background geometry and matter, which satisfies Einstein's equation during the inflational process, will inevitably lead to the existence of an initial singularity [7, 8]. Yet, the inflation paradigm in general ignores the pre-inflationary dynamics and simply sets the initial condition of the perturbations in the Bunch-Davies vacuum at the onset of the slow-roll epoch. To resolve any of these problems, the ultraviolet (UV) physics is needed.

So far, various approaches have been proposed to study the aforementioned effects; see, for example, [5–11], and references therein. In most of such considerations, both scalar and tensor perturbations produced during the inflationary epoch are governed by the equation

$$\mu_k''(\eta) + \left(\omega_k^2(\eta) - \frac{z''}{z}\right)\mu_k(\eta) = 0, \tag{1.1}$$

where $\mu_k(\eta)$ denotes the mode function of inflationary perturbations, and a prime indicates differentiation with respect to the conformal time η. k is the comoving wave number, and $z = z(\eta)$ depends on the background and the types of perturbations (scalar and tensor). In the present paper, we will consider the particular nonlinear dispersion relation

$$\omega_k^2(\eta) = k^2\left[1 - \hat{b}_1\left(\frac{k}{aM_*}\right)^2 + \hat{b}_2\left(\frac{k}{aM_*}\right)^4\right], \tag{1.2}$$

where M_* is the relevant energy scale of the nonlinear dispersion relation, $a = a(\eta)$ is the scale factor of the background universe, and $\hat{b}_1$ and $\hat{b}_2$ are dimensionless constants. In order to get a healthy ultraviolet limit if $\hat{b}_1 \neq 0$, one in general requires $\hat{b}_2 > 0$. When $\hat{b}_1 = 0 = \hat{b}_2$, it reduces to that of general relativity.

The nonlinear dispersion relation in Eq. (1.2) was first suggested for inflationary perturbations in [5] as a toy model, which has been used to study the unknown effects of trans-Planckian physics. Later it was found that it could be naturally realized in the framework of Hořava-Lifshitz theory of gravity [12, 13]. While the last two terms on the right hand side of Eq. (1.2) denote the contributions from the fourth and sixth-order spatial operators in the theory of Hořava-Lifshitz gravity,

* Tao_Zhu@baylor.edu
† anzhong_wang@baylor.edu
‡ klaus_kirsten@baylor.edu
§ gerald_cleaver@baylor.edu
¶ qin_sheng@baylor.edu

the term ω_k^2 comes from the fact that the theory only allows the second-order time derivative operators. The essential point of keeping the time derivative operators to the second-order and the high-dimensional spatial operators up to the sixth-order is that it not only reserves the unitarity of the theory, but also makes the theory power-counting renormalizable.

To have a better physical understanding of the quantum gravitational effects, it is highly desirable to solve Eq.(1.1) analytically for the nonlinear dispersion relation (1.2), and then extract information from it, including the power spectra, spectral indices and runnings. Such studies are very challenging, as the problem becomes so mathematically involved, and meanwhile the treatment needs to be sufficiently accurate, in order to identify precisely such effects and seek observational signatures in the current and forthcoming experiments. Recently, we developed a powerful and effective method, *the uniform asymptotic approximation* to accurately construct analytical solutions of the mode function with a nonlinear dispersion relation [14]. It should be noted that the uniform asymptotic approximation was first applied to inflationary cosmology by Habib *et al.* [15], in which the dispersion relation is the standard linear relation $\omega_k(\eta) = k^2$, where the equation of motion only has one single turning point (see also [12]). We generalized the method of Habib *et al.* to the case with the nonlinear dispersion relation of Eq.(1.2), where multiple and high-order turning points are allowed. Furthermore, we extended the first-order uniform asymptotic approximation to the third-order in cases where there exists only one-turning point [16]. The formulas were then applied to k-inflationary models [17] as well as to the ones in loop quantum cosmology (LQC) with holonomy and inverse-volume corrections [18].

The aim of this paper is to generalize our studies carried out in [14] from the first-order to the third-order approximations with any number and order of turning-points for the dispersion relation given by Eq.(1.2). Up to the third-order, the upper bounds of errors are $\lesssim 0.15\%$ [16], which are accurate enough for the current and forthcoming experiments [19]. We emphasize that the method to be developed in this paper is quite general, and can easily be extended to other inflationary models with different quantum gravitational effects. To proceed further, we assume that the background evolution with an inflationary scalar field satisfies the usual Friedmann and Klein-Gordon equations [1],

$$H^2 = \frac{1}{3M_{\rm Pl}^2}\left(\frac{1}{2}\dot{\phi}^2 + V(\phi)\right), \tag{1.3}$$

$$\ddot{\phi} + 3H\dot{\phi} + \frac{dV(\phi)}{d\phi} = 0, \tag{1.4}$$

where $H \equiv \dot{a}/a$ is the Hubble parameter, $V(\phi)$ is the potential of the inflation field ϕ, and $M_{\rm Pl}$ is the reduced Planck mass. In the above, a dot represents the derivative with respect to the cosmic time t, which in terms of the conformal time is given as

$$\eta(t) = \int_{t_{\rm end}}^{t} \frac{dt'}{a(t')}. \tag{1.5}$$

Here $t_{\rm end}$ is the cosmic time when the inflation ends.

In addition, an important feature of the nonlinear dispersion relation is that it could produce additional excited states for primordial perturbations on the sub-horizon scale during inflation. This has been extensively studied in [20, 21]. In general, the solution of Eq.(1.1) has the following form in the sub-horizon regime $H \ll k/a \ll M_*$ (in the leading WKB approximation),

$$\mu_k(\eta) = \frac{1}{\sqrt{2\omega_k(\eta)}}\left(\tilde{\alpha}_k e^{-i\int \omega_k d\eta} + \tilde{\beta}_k e^{i\int \omega_k d\eta}\right), \tag{1.6}$$

where $\tilde{\alpha}_k$ and $\tilde{\beta}_k$ satisfy the relation

$$|\tilde{\alpha}_k|^2 - |\tilde{\beta}_k|^2 = 1. \tag{1.7}$$

Usually, $\tilde{\beta}_k = 0$ if the mode starts at the Bunch-Davies vacuum and the coefficient term $\Omega_k^2(\eta) = \omega_k^2(\eta) - z''/z$ in Eq. (1.1) satisfies the adiabatic condition

$$\left|\frac{3(\Omega_k')^2}{4\Omega_k^4} - \frac{\Omega_k''}{2\Omega_k^3}\right| \ll 1, \tag{1.8}$$

from the onset of inflation until the sub-horizon regime. However, if the adiabatic condition is violated in the region when $k/a \gtrsim M_*$, then the primordial perturbation modes through this region will lead to a nonzero $\tilde{\beta}_k$. This immediately raises the question whether the back-reaction of such additional excited state (i.e., $\tilde{\beta}_k$ mode) is small enough to allow inflation to last long enough. Such a consideration leads to the following constraint [21],

$$|\tilde{\beta}_k|^2 \ll 8\pi \frac{M_{\rm Pl}^2 H_{\rm inf}^2}{M_*^4}, \tag{1.9}$$

where $H_{\rm inf}$ is the Hubble constant when the inflation just starts. Note that similar constraints can also be found in [22]. In the current paper, with the approximate solutions obtained by using the high-order uniform asymptotic approximation to be developed below, we are able to determine the coefficient $\tilde{\beta}_k$ explicitly, so that we can estimate the effects of the back-reactions on the primordial spectra precisely.

The rest of this paper is organized as follows. In Appendix A, we systematically develop the high-order uniform asymptotic approximation method for multi-turning points, and expand the mode function in terms of $1/\lambda$ to an arbitrarily high order, in which the error bounds are given in each order of the approximation, where $\lambda \gg 1$. Then in Appendix B, we consider

[1] This assumption is not essential, and can be easily generalized to the case where the evolution of the background is affected by quantum gravitational corrections. Such corrections could lead to non-slow-roll inflation, such as the case in LQC [18]. However, the uniform asymptotic approximation method is not restricted to slow-roll inflationary models, and can be thus in principle equally applied to the non-slow-roll case.

the matching of individual approximate solutions constructed in Appendix A. By applying the formalism developed in Appendices A and B to inflationary perturbation modes with the above nonlinear dispersion relation, in Sec. II, we obtain the general expressions of the power spectra to the third-order from the analytically approximate mode function obtained in the uniform asymptotic approximation. Then, we investigate the constraints on the Bogoliubov coefficient $\tilde{\beta}_k$, in order for the inflation to last longer enough. In Sec. III, we investigate features of the power spectra, and study their potential applications to certain inflationary models. In particular, we show that, even with the aforementioned constraints, the model with a quadratic potential can be reconciled with observations after the quantum gravitational corrections are taken into account. Our main conclusions are summarized in Sec. IV.

II. SPECTRA OF PRIMORDIAL PERTURBATIONS

A. Turning Points and WKB Approximation

The evolutions of both scalar and tensor perturbations, which obey the equation of motion (1.1), depend on both the background of the Universe and the nonlinear dispersion relations (1.2). With the assumption of the slow-roll evolution of the background, then the behaviors of the mode are very sensitive to the signs of $\omega_k^2(\eta) - z''/z$ in Eq. (1.1). When $\omega_k^2(\eta) \gg |z''/z|$, the solution is of the type of oscillation,

$$\mu_k(\eta) \sim e^{\pm i \int \omega_k(\eta) d\eta}, \tag{2.1}$$

and when $\omega_k^2(\eta) \ll |z''/z|$, it is of the form,

$$\mu_k(\eta) \sim \frac{\alpha_1}{z(\eta)} + \alpha_2 z(\eta). \tag{2.2}$$

Here we note that the former corresponds to solutions in the region where the adiabatic condition (1.8) is fulfilled. Then, the problem of obtaining the solution of Eq. (1.1) thus reduces to solving the equation in the intermediate regions when $\omega_k^2(\eta) \sim |z''/z|$. In these regions, the signs of $\Omega_k^2(\eta) \left[\equiv \omega_k^2(\eta) - z''/z\right]$ change. As a result, the solution will change from that of oscillation to that of decaying/growing, or vice versa. The transition point where $\Omega_k^2(\eta) = 0$ is usually called a *turning point*. As shown above, the solution of the mode function has quite different behaviors in different sides of the turning point. In particular, in the region where $\Omega_k^2(\eta) \simeq 0$, the adiabatic condition (1.8) is broken down, as shown explicitly in Fig. 1, and then the usual WKB approximation becomes invalid. Therefore, in order to determine the solution of Eq. (1.1) in the whole phase space, other approximations near the turning points are required. To this purpose, in the following we shall show how one can solve Eq. (1.1) at these turning points by using the uniform asymptotic approximation.

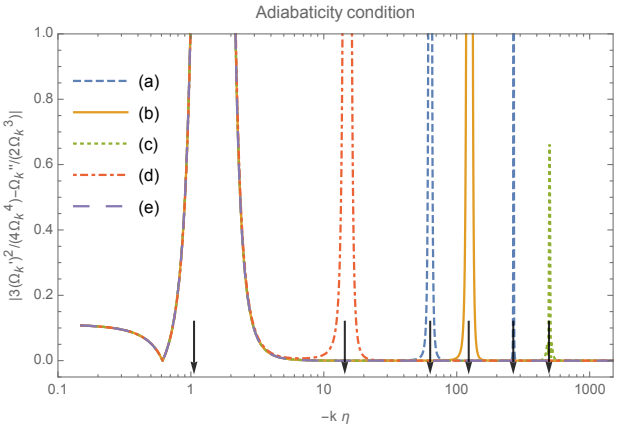

FIG. 1. The adiabatic condition of Eq. (1.8) for the WKB approximation is violated at the turning points $\Omega_k^2(\eta) \equiv \omega_k^2(\eta) - z''/z = 0$, denoted by the down-pointing vertical arrows. The curves (a), (b), (c), (d) and (e) correspond, respectively, to the cases illustrated in Fig. 2.

B. Approximate Solutions near Turning Points

The uniform asymptotic approximation provides a systematic and effective method to construct accurate solutions near turning points. To show this, let us re-write Eq.(1.1) in the form [23, 24],

$$\frac{d^2\mu_k(y)}{dy^2} = \left[\lambda^2 \hat{g}(y) + q(y)\right]\mu_k(y), \tag{2.3}$$

where the new variable $y(\equiv -k\eta)$ is dimensionless, and

$$\begin{aligned}\lambda^2 \hat{g}(y) + q(y) &\equiv -\frac{1}{k^2}\left(\omega_k^2(\eta) - \frac{z''}{z}\right) \\ &= \frac{\nu^2 - 1/4}{y^2} - 1 + b_1\epsilon_*^2 y^2 - b_2\epsilon_*^4 y^4,\end{aligned} \tag{2.4}$$

where $\nu^2 \equiv 1/4 + \eta^2 z''/z$, $b_1 = \hat{b}_1/(a^2H^2\eta^2)$, $b_2 = \hat{b}_2/(a^4H^4\eta^4)$, and $\epsilon_* = H/M_*$. In the above, the quantity $z = z(\eta)$ depends on the types of perturbations. In particular, for scalar perturbations we have $z_s(\eta) = a\dot{\phi}/H$ and for tensor perturbations we have $z_t(\eta) = a$. Restricting to the slow-roll evolution of the background, as we have assumed in this paper, we have $b_1 = (1 + 2\epsilon_1 + \mathcal{O}(\epsilon^2))\hat{b}_1$, $b_2 = (1 + 4\epsilon_1 + \mathcal{O}(\epsilon^2))\hat{b}_2$, $\nu = 3/2 + \epsilon_1 + \epsilon_2/2 + \mathcal{O}(\epsilon^2)$ for scalar perturbations, and $\nu = 3/2 + \epsilon_1 + \mathcal{O}(\epsilon^2)$ for tensor perturbations with $\epsilon_1 \equiv -\dot{H}/H^2$, $\epsilon_2 \equiv d\ln\epsilon_1/d\ln a$, where ϵ_i denote the slow-roll parameters at the first-order slow-roll approximation.

Note that Eq. (2.4) cannot determine the two functions $g(y)$ and $q(y)$ uniquely. A fundamental reason to introduce two of them is to have one extra degree of freedom, so later we are allowed to choose them in such a way that the error control functions, associated with the uniform asymptotic approximation, can be minimized.

The convergence of these error control functions are very sensitive to their behaviors near the poles (singularities) of the function $\lambda^2\hat{g}(y)$, as we have discussed in details in Appendix A. From the expression of Eq. (2.4), one can see that there are two poles, one is located at $y = 0^+$ and the other is at $y = +\infty$. Now one can follow the guidance summarized in the last paragraph in Appenxia. A to determine the functions $\lambda^2\hat{g}(y)$ and $q(y)$.

The guidance to determine the functions $\lambda^2\hat{g}(y)$ and $q(y)$ contains three conditions. The first condition requires that near the two poles we must have $|q(y)| < |\lambda^2\hat{g}(y)|$, which in turn requires that $\lambda^2\hat{g}(y)$ must be of the second-order at the pole $y = 0^+$, and of the fourth-order at the pole $y = +\infty$. Then, the second condition requires that the functions $\lambda^2\hat{g}(y)$ and $q(y)$ must be chosen as

$$\begin{aligned} q(y) &= -\frac{1}{4y^2} + \frac{q_1}{y} + q_2 + q_3 y + q_4 y^2 + q_5 y^3 + q_6 y^4, \\ \lambda^2\hat{g}(y) &= \frac{\nu^2}{y^2} - \frac{q_1}{y} - (1+q_2) - q_3 y \\ &\quad + (b_1\epsilon_*^2 - q_4) y^2 - q_5 y^3 - (b_2\epsilon_*^4 + q_6) y^4, \end{aligned} \tag{2.5}$$

where q_i with $i = 1, 2, 3, 4, 5, 6$ are constants. Considering the third condition one concludes that the pole $y = +\infty$ of $q(y)$ must have order less than one, thus $q_i = 0$ with $i > 2$. One can choose $q_{1,2} = 0$ for the sake of simplicity. Then, the functions $\lambda^2\hat{g}(y)$ and $q(y)$ finally take the form

$$q(y) = -\frac{1}{4y^2}, \tag{2.6}$$

$$\lambda^2\hat{g}(y) = \frac{\nu^2}{y^2} - 1 + b_1\epsilon_*^2 y^2 - b_2\epsilon_*^4 y^4. \tag{2.7}$$

Clearly, the function $\lambda^2\hat{g}(y)$ is free of singularities within the range $y \in (0, +\infty)$.

Except the two poles at $y = 0^+$ and $y = +\infty$, $\lambda^2\hat{g}(y)$ in general has three zeros for $y \in (0, +\infty)$, which depends on the three parameters b_1, b_2, and ϵ_*. The zeros of $\lambda^2\hat{g}(y)$ are also called turning points of the second-order differential equation (2.3). These turning points can be determined by solving the equation $\lambda^2\hat{g}(y) = 0$, which are,

$$\begin{aligned} y_0 &= \left\{ \frac{b_1}{3b_2\epsilon_*^2} \left[1 - 2\sqrt{1-\mathcal{Y}} \cos\left(\frac{\theta}{3}\right) \right] \right\}^{1/2}, \\ y_1 &= \left\{ \frac{b_1}{3b_2\epsilon_*^2} \left[1 - 2\sqrt{1-\mathcal{Y}} \cos\left(\frac{\theta+2\pi}{3}\right) \right] \right\}^{1/2}, \\ y_2 &= \left\{ \frac{b_1}{3b_2\epsilon_*^2} \left[1 - 2\sqrt{1-\mathcal{Y}} \cos\left(\frac{\theta+4\pi}{3}\right) \right] \right\}^{1/2}, \end{aligned} \tag{2.8}$$

with $\mathcal{Y} \equiv 3b_2/b_1^2$ and

$$\theta \equiv -\left(1 - \frac{3}{2}\mathcal{Y} + \frac{3}{2}b_1\mathcal{Y}^2\nu^2\epsilon_*^2\right)(1-\mathcal{Y})^{-3/2}. \tag{2.9}$$

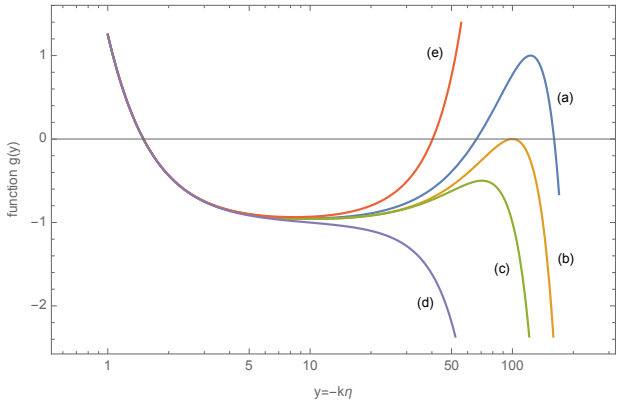

FIG. 2. The function $g(y) = \lambda^2\hat{g}(y)$ defined in Eq.(2.7): (a) Three different and single real roots of the equation $\lambda^2\hat{g}(y) = 0$. (b) One single real root and one double real root. (c) One single real root and two complex roots. (d) One single real root. (e) Two single real roots when $\hat{b}_2 < 0$. The turning points y_0, y_1, and y_2 are all real and positive in Case (a).

Depending on the signs of Δ, where

$$\Delta \equiv (\mathcal{Y}-1)^3 + \left(1 - \frac{3}{2}\mathcal{Y} + \frac{3}{2}b_1\mathcal{Y}^2\nu^2\epsilon_*^2\right)^2, \tag{2.10}$$

the nature of the three roots is different. In Fig. 2, we display five different cases for the function $\lambda^2\hat{g}(y)$, corresponding to different types of roots [2]. When $\Delta < 0$, the three roots (y_0, y_1, y_2) are all real and different, which corresponds to Case (a) in Fig. 2. When $\Delta = 0$, there are one single real root y_0 and one double real root y_1 ($y_1 = y_2$), which corresponds to Case (b) in Fig. 2. When $\Delta > 0$, there are one single root y_0 and two complex conjugated roots y_1 and y_2 with $y_1* = y_2$, which corresponds to Cases (c) and (d) in Fig. 2. The difference between Case (c) and Case (d) is that for Case (d), the two complex roots are largely spaced in the imaginary axis, and as we shall show later, we can treat this case as it has only one single real root. We also display a special Case (e) in Fig. 2 by taking $\hat{b}_2 < 0$, which has two real turning points. Note that throughout this paper we assume $y_0 < \mathrm{Re}(y_1) \leq \mathrm{Re}(y_2)$.

The performance of the uniform asymptotic approximation for different types of turning points are different. The treatment for the single real turning point is presented in Appendix. A 3, while the treatment for a pair of turning points which could be either both single, double, or both complex is presented in Appendix. A 4. For the single real turning point y_0, following the procedure in Appendix. A 3, one can construct the approximate so-

[2] It should be noted that in [14] Cases (c) and (d) were considered as one, while Case (e) was limited by requiring that the mode be stable at the UV.

lution of Eq. (1.1) for primordial perturbation modes as

$$\mu_k(y) = \left(\frac{\xi(y)}{\hat{g}(y)}\right)^{1/4} U(\xi), \tag{2.11}$$

where $\xi(y)$ is a growing function of y in the range $y \in (0^+, \mathrm{Re}(y_1))$ given by Eq. (A.32) and $U(\xi)$ is expanded in terms of Airy function in Eq. (A.45).

For a pair of turning points y_1 and y_2, as we discussed above, they could be either both single real, double, or even complex. In the uniform asymptotic approximation, as we have shown in Appendix. A 4, we can treat them together. Following the procedure in Appendix. A 4, the corresponding solution of Eq. (1.1) now can be expressed as

$$\mu_k(y) = \left(\frac{\zeta(y)^2 - \zeta_0^2}{-\hat{g}(y)}\right)^{\frac{1}{4}} U(\zeta), \tag{2.12}$$

where $\zeta(y)$ is a decaying function of y in the range of $y \in (y_0, +\infty)$, which is given by Eqs. (A.51, A.53, A.55, A.57) respectively for different cases, ζ_0^2 is defined in Eq. (A.49), and $U(\zeta)$ is expressed in terms of parabolic cylinder functions in Eq. (A.71).

Then imposing the adiabatic vacuum state in the limit $y \to +\infty$ as in Eq. (B.1), and matching the individual solutions in Eq. (2.11) and Eq. (2.12) in their overlaping region $y \in (y_0, \mathrm{Re}(y_1)$, the behaviors of the solution of the primordial perturbations modes during the whole region $y \in (0^+, +\infty)$ now can be completely determined.

As the construction of the approximate solutions in the uniform asymptotic approximation are very much mathematically involved, in this paper we leave most of the mathematical derivations into Appendix. A and Appendix. B. In Appendix. A, we provide a general and self-contained introduction to the uniform asymptotic approximation and illustrate how to construct accurate solutions for different types of turning points. In Appendix. B, we show how to match the individual solutions in different regions so that we can get a solution in the whole spacetime.

C. Spectra of Primordial Perturbations

Now with the approximate solutions of Eq. (2.11) and Eq. (2.12), we are in the position to calculate the spectra of both scalar and tensor perturbations. In order to do so, we consider the limit $y \to 0^+$, for which only the growing mode of the approximate solution is relevant. Considering the asymptotic form of the Airy functions in the limit $y \to 0^+$ (i.e., $\xi(y) \to +\infty$), we have [16]

$$\lim_{y\to 0^+} \mu_k(\eta) = \frac{\beta_0 e^{\frac{2}{3}\xi^{2/3}}}{\lambda^{1/6}\hat{g}^{1/4}\pi^{1/2}}\left[1 + \frac{\mathscr{H}(+\infty)}{2\lambda} + \frac{\mathscr{H}^2(+\infty)}{8\lambda^2} + \mathcal{O}\left(\frac{1}{\lambda^3}\right)\right], \tag{2.13}$$

where $\mathscr{H}(\xi)$ is the error control function associated with the approximate solution at the turning point y_0 and the coefficient β_0 is determined in Eq. (B.24). Then, the power spectra read

$$\begin{aligned}\Delta^2(k) &\equiv \frac{k^3}{2\pi^2}\left|\frac{\mu_k(y)}{z(\eta)}\right|^2_{y\to 0^+} \\ &\simeq \mathscr{A}(k)\frac{k^2}{4\pi^2}\frac{-k\eta}{z^2(\eta)\nu(\eta)}\exp\left(2\lambda\int_y^{y_0}\sqrt{\hat{g}(y')}dy'\right) \\ &\quad\times\left[1 + \frac{\mathscr{H}(+\infty)}{2\lambda} + \frac{\mathscr{H}^2(+\infty)}{8\lambda^2} + \mathcal{O}\left(\frac{1}{\lambda^3}\right)\right],\end{aligned} \tag{2.14}$$

where $\mathscr{A}(k)$ denotes the modified factor due to the presence of the turning points y_1 and y_2, which reads

$$\begin{aligned}\mathscr{A}(k) &= 1 + 2e^{\pi\lambda\zeta_0^2} + 2e^{\pi\lambda\xi_0^2/2}\sqrt{1 + e^{\pi\lambda\zeta_0^2}} \\ &\quad\times\left\{\cos 2\mathfrak{B} - \frac{\mathscr{I}(\zeta) + \mathscr{H}(\xi)}{\lambda}\sin 2\mathfrak{B}\right. \\ &\quad\left. - \frac{\left[\mathscr{I}(\zeta) + \mathscr{H}(\xi)\right]^2}{2\lambda^2}\cos 2\mathfrak{B}\right\}.\end{aligned} \tag{2.15}$$

Here $\mathscr{I}(\zeta)$ is the error control function associated with the approximate solution at the turning points y_1 and y_2, and the quantity $\mathscr{B}$ is given by Eq. (B.25).

The quantity ζ_0^2 measures the quantum effects of the nonlinear dispersion relation. When ζ_0^2 is positive and large, which corresponds to the case that both y_1 and y_2 are real [i.e. Case (a) in Fig. 2 with the condition that y_1 and y_2 are largely spaced], one finds

$$e^{\pi\lambda\zeta_0^2} \gg 1, \tag{2.16}$$

thus the power spectrum is exponentially enhanced. When $\zeta_0^2 = 0$, which corresponds to the case that the turning points satisfy $y_1 = y_2$, i.e. Case (b) in Fig. 2, one finds

$$\begin{aligned}\mathscr{A} &= 3 + 2\sqrt{2}\left\{\cos 2\mathfrak{B} - \frac{\mathscr{I}(\zeta) + \mathscr{H}(\xi)}{\lambda}\sin 2\mathfrak{B}\right. \\ &\quad\left. - \frac{\left[\mathscr{I}(\zeta) + \mathscr{H}(\xi)\right]^2}{2\lambda^2}\cos 2\mathfrak{B}\right\}.\end{aligned} \tag{2.17}$$

For the case ζ_0 is negatively large, which corresponds to the case when the turning points y_1 and y_2 are complex conjugate and largely spaced in the imaginary axis, that is, Case (d) in Fig. 2, one has

$$e^{\pi\lambda\zeta_0^2} \ll 1. \tag{2.18}$$

Thus, the power spectrum reduces to the usual one with only one single turning point y_0, which has been calculated in detail in [16] up to the third-order approximation.

With the above expression of the power spectrum, the corresponding spectral index can be calculated as

$$n_{s,t} = \frac{d\ln \mathscr{A}_{s,t}(k)}{d\ln k} + n_{s,t}^{(one)}, \tag{2.19}$$

where $n_{s,t}^{(one)}$ is the spectral index when $\lambda^2\hat{g}(y)$ has only one turning point, and its explicit expression is given in [16]. When ζ_0^2 is negative and large, $\mathscr{A}_{s,t}$ reduces to one, and thus the first term in Eq.(2.19) reduces to zero. This is consistent with the discussions given in the last paragraph. More specifically, for the first-order approximation the modified factor is only a function of ζ_0^2 and $\mathfrak{B}$, and we can write the spectral index in a more explicit form

$$n_{s,t} = \frac{\partial \ln \mathscr{A}_{s,t}}{\partial \zeta_0^2}\frac{d\zeta_0^2}{d\ln k} + \frac{\partial \ln \mathscr{A}_{s,t}}{\partial \mathfrak{B}}\frac{d\mathfrak{B}}{d\ln k} + n_{s,t}^{(one)}, \tag{2.20}$$

where

$$\frac{d\zeta_0^2}{d\ln k} \equiv \frac{2}{\pi}\frac{d}{d\ln k}\int_{y_1}^{y_2}\sqrt{\hat{g}(y')}dy', \tag{2.21}$$

and

$$\frac{d\mathfrak{B}}{d\ln k} \equiv \lambda\frac{d}{d\ln k}\int_{y_0}^{\mathrm{Re}(y_1)}\sqrt{-\hat{g}(y')}dy' + \frac{\lambda}{\pi}\phi'\left(\frac{\lambda}{2}\zeta_0^2\right)\frac{d}{d\ln k}\int_{y_1}^{y_2}\sqrt{\hat{g}(y')}dy', \tag{2.22}$$

in which $\phi(x)$ is given by Eq.(C.6) and $\phi'(x) \equiv d\phi(x)/dx$. Here we would like to mention that the above formulas are very general and can be applied to any dispersion relation which has three turning points.

Some remarks about the terminologies are in order. In general, the function $\lambda^2\hat{g}(y)$ in Eq.(2.7) has three turning points y_0, y_1, and y_2, as we already have shown in Fig. 2. In order to apply the uniform asymptotic approximation to the turning point y_0, we have imposed the conditions: (i) $|q(y)|$ *is small compared with* $|\lambda^2\hat{g}(y)|$, *except in the neighborhoods of* y_0 *where it is small compared with* $|\lambda^2\hat{g}(y)(y-y_0)^{-1}|$. (ii) *At the turning points* y_1 *and* y_2, $|q(y)|$ *is small compared with* $|\lambda^2\hat{g}(y)|$, *except in the neighborhoods of* y_1 *and* y_2 *where it is small compared with* $|\lambda^2\hat{g}(y)(y-y_1)^{-1}(y-y_2)^{-1}|$. In general the first condition does not hold in the neighborhoods of y_1 and y_2 [Cases (a), (b) and (c) as shown in Fig. 2], except for the case that y_1 and y_2 are complex and largely spaced in the complex plane, which is Case (d) as shown in Fig. 2. In the latter, one can consider that the function $\lambda^2\hat{g}(y)$ has one turning point in the whole range of y, and as we already showed above, the result obtained with three-turning points exactly reduces to the result obtained with one-turning point. Therefore, when we consider that the function $\lambda^2\hat{g}(y)$ only has one-turning point, we mean that condition (i) holds everywhere in the whole range of our interest, which is Case (d) in Fig. 2.

D. Back-reaction of quantum gravitational effects

As we have mentioned in the introduction, in general the nonlinear dispersion relation leads to the productions of particles. This raises an important question, namely whether or not the back-reaction of the excited modes is small enough to allow inflation to last longer enough. In order to clarify this point, let us consider the approximate solution in the sub-horizon region $H < k/a < M_*$ (equivalently for the region $y_0 \ll y \ll \mathrm{Re}(y_1)$)), during which the approximate solution takes the form as Eq. (B.20). In the sub-horizon region, as $\omega_k^2 \gg z''/z$, thus one has $\lambda^2\hat{g}(y) \simeq -\omega_k^2/k^2$ and

$$\lambda\int_{y_0}^{y}\sqrt{-\hat{g}}dy' \simeq -\int_{\eta_0}^{\eta}\omega_k(\eta)d\eta, \tag{2.23}$$

then the solution in Eq. (B.20) can be simplified into the form

$$\mu_k(\eta) \simeq \frac{\lambda^{1/3}}{\sqrt{2\omega_k}}\sqrt{\frac{k}{2\pi}}\left(A - i\frac{\bar{B}}{\lambda}\right) \times\Big\{(\alpha_0+i\beta_0)e^{i\int_{\eta_0}^{\eta}\omega_k d\eta' - \frac{\pi}{4}} + (\alpha_0 - i\beta_0)e^{-i\int_{\eta_0}^{\eta}\omega_k d\eta' + \frac{\pi}{4}}\Big\}, \tag{2.24}$$

where $A = A(\lambda,\xi)$, $\bar{B}(\lambda,\xi)/\lambda$ are given by Eq. (B.22), and α_0, β_0 are given by Eq.(B.24). From the above analytical approximate solutions, one can identify the Bogoliubov coefficient of the excited modes at the sub-horizon scales as,

$$\frac{|\tilde{\beta}_k|^2}{\lambda^{2/3}} = \frac{k}{2\pi}\left|A - i\frac{\bar{B}}{\lambda}\right|^2|\alpha_0 + i\beta_0|^2. \tag{2.25}$$

By using Eq. (B.22) one can obtain that

$$\left|A - i\frac{\bar{B}}{\lambda}\right|^2 \simeq 1 + \mathcal{O}(1/\lambda^3), \tag{2.26}$$

thus up to the third-order approximation in the uniform asymptotic approximation, one finds

$$\frac{|\tilde{\beta}_k|^2}{\lambda^{2/3}} = \frac{k}{2\pi}\Big[|\alpha_0|^2 + |\beta_0|^2 + i(\alpha_0^*\beta_0 - \alpha_0\beta_0^*)\Big]. \tag{2.27}$$

In order to avoid large back-reactions [cf. Eq.(1.9)], one has to impose the condition [21],

$$|\tilde{\beta}_k|^2 \lesssim 8\pi\frac{H_{\mathrm{inf}}^2 M_{\mathrm{Pl}}^2}{M_*^4}, \tag{2.28}$$

where H_{inf} is the energy scale of the inflation and the Planck 2015 data yields the constraint $H_{\mathrm{inf}}/M_{\mathrm{Pl}} \leq 3.5\times 10^{-5}$ [4]. Thus if we take $H_{\mathrm{inf}}/M_* \sim 2\times 10^{-3}$, one can infer that

$$|\tilde{\beta}_k|^2 \lesssim \mathcal{O}(1). \tag{2.29}$$

For smaller M_*, the Bogoliubov coefficient $|\tilde{\beta}_k|^2$ can be larger [3]. But here we shall take the above limit and derive the constraints on $\mathscr{A}_{s,t}$. Since the modified factor in general can be expressed as

$$\mathscr{A} \simeq |\tilde{\alpha}_k + \tilde{\beta}_k|^2, \tag{2.30}$$

it is easy to obtain that

$$\sqrt{1+|\tilde{\beta}_k|^2} - |\tilde{\beta}_k| \lesssim \sqrt{\mathscr{A}} \lesssim |\tilde{\beta}_k| + \sqrt{1+|\tilde{\beta}_k|^2}. \tag{2.31}$$

Then, Eq.(2.29) places constraints on the modified factor $\mathscr{A}_{s,t}$ for both of the primordial scalar and tensor perturbations as

$$3 - 2\sqrt{2} \lesssim \mathscr{A}_{s,t} \lesssim 3 + 2\sqrt{2}. \tag{2.32}$$

III. MAIN FEATURES OF THE SPECTRA

One natural question is whether the quantum gravitational effects could produce some non-trivial features in the spectra of the primordial perturbations. In this section, we shall point out some of these features that could be observationally interesting.

A. Nearly scale-invariance of the primordial perturbations

We consider the nonlinear dispersion relation with

$$b_1 = (1 + \mathcal{O}(\epsilon))\, \hat{b}_1, \tag{3.1}$$

$$b_2 = (1 + \mathcal{O}(\epsilon))\, \hat{b}_2, \tag{3.2}$$

where ϵ represents the slow-roll parameter. From these expressions we see that if we expand the perturbations spectra about a pivot scale $k_\star$, the derivative of all the above quantities only contributes to the second-order of the slow-roll approximations or to the order $\mathcal{O}(\epsilon) \times \epsilon_*^2$ for the ϵ_* term. So if we only consider the first-order slow-roll expansion (ignore the term $\mathcal{O}(\epsilon) \times \epsilon_*^2$ as well), the spectral indices will be the same as for the case that $\lambda^2 \hat{g}(y)$ only has one turning point, in which the quantum gravitational effects contribute only small corrections to the spectral index of GR. Thus, even after the quantum gravitational effects are taken into account, in this case the primordial spectra are still nearly scale-invariant.

This is important. As discussed in the second reference of [6], the authors have imposed two additional conditions, the adiabatic condition (i.e., condition when Eq.(1.8) holds) and the separation of the scale (i.e., $\epsilon_* \ll 1$), to justify the scale invariance of the power spectra. With these two conditions, the evolution of inflationary modes which starts at an initial Bunch-Davies vacuum must trace the adiabatic state during inflation until the mode crosses the Hubble horizon. This exactly corresponds to the one turning point case we discussed above [Case (d) as shown in Fig. 2]. If the adiabatic condition is violated in an intermediate region during inflation, then the equation of the mode function may have more than one turning point [in fact three turning points as shown in Fig. 2 for Cases (a), (b), and (c)]. In these cases, the initial Bunch-Davies vacuum shall evolve into a mixed state as shown in Eq.(1.6) with a non-zero Bogoliubov coefficient $\tilde{\beta}_k$ even when the adiabatic condition is restored before these modes leave the Hubble horizon. Our results show that even with such mixed state, the property of almost scale-invariance of the primordial spectrum still remains.

In addition to the above possibilities, there still exist cases in which strong scale-dependence of primordial spectrum may occur. For example, the adiabatic condition may be violated at the initial time. In particular, this is the case when $\hat{b}_2 < 0$, Case (e) as shown in Fig. 2. In such a case, we cannot choose the initial state as the usual Bunch-Davies vacuum. In the first reference of [6], the authors considered the case in which the initial state is determined by minimizing the energy density. For such an initial state, it was found that significant deviations from the scale-invariant spectrum can be obtained. However, as we already pointed out in the Introduction, a healthy ultraviolet limit requires $\hat{b}_2 > 0$, thus scale invariance is protected by a stability requirement of the underlying theory in the UV.

Moreover, even if a healthy ultraviolet limit is guaranteed, the scale-invariance of the spectrum could still be changed dramatically when different initial conditions are chosen. For example, it was shown that the power spectrum could be strongly scale-dependent when one chooses an instantaneous Minkowski vacuum, see the first reference of [6] for details.

B. Oscillations of the primordial perturbation spectra

Another important effect from the quantum gravitational corrections is that they generically lead to oscillations in the primordial perturbation spectra [7], as one can see clearly from our analytical expression (2.14). Roughly, the phase of the oscillations can be expanded at the pivot scale $k_\star$ in the form,

$$2\mathfrak{B}(k) \simeq 2\mathfrak{B}(k_\star) + \mathcal{O}(\epsilon^2) \times \ln\frac{k}{k_\star}. \tag{3.3}$$

It shows clearly that the second term in the expansion is at the second-order in slow-roll approximation, which indicates that the k-dependence is extremely weak, and

[3] For example, in the healthy extension of the Hořava theory [25], solar system tests lead to $M_* \lesssim 10^{16}$GeV [26].

thus it might be very difficult to observe it in the current and forthcoming experiments. In this sense, the cosine function in Eq. (2.14) affects only the overall amplitude in primordial spectrum, rather than produces a k-dependent oscillatory pattern in the primordial spectrum. It must be noted that the underlying assumption of such a conclusion is that the initial state is the Bunch-Davies vacuum. Similar to the cases studied in the first reference of [6], choosing the initial state as an instantaneous Minkowski vacuum could lead to scale-dependent oscillations in the power spectra that could be observationally significant. But, as we mentioned above, this will also lead to significant derivations of scale-invariance of the power spectra.

C. Modifications of Power Spectra

In addition, the quantum gravitational effects generically modify the primordial spectra, depending on the coupling constants $\hat{b}_1$ and $\hat{b}_2$, where the values of these parameters depend on the types of perturbations, tensor or scalar [12]. This will in turn affect the ratio r between the tensor and scalar power spectra, which could lead to observational consequences, and bring the theory directly under tests. For example, in GR the inflationary model with a quadratic potential predicts,

$$r_{\rm GR} \equiv \frac{8\Delta^{(t)2}_{\rm GR}(k_\star)}{\Delta^{(s)2}_{\rm GR}(k_\star)} \sim 0.13, \tag{3.4}$$

which is obviously in tension with the upper bound obtained recently by Planck 2015, $r_{\rm Planck} \leq 0.11$ at 95% C.L. [4]. However, if we take quantum gravitational effects into account, the tension could disappear completely, as now we have,

$$r \equiv \frac{8\Delta^{(t)2}(k_\star)}{\Delta^{(s)2}(k_\star)} = \left(\frac{\mathscr{A}_t}{\mathscr{A}_s}\right) r_{\rm GR}. \tag{3.5}$$

Thus, by properly choosing the coupling constants $\hat{b}^{(t,s)}_A$ $(A = 1, 2)$, one has various ways to rescue the quadratic model, for example, by suppressing $\mathscr{A}_t$ and/or enlarging $\mathscr{A}_s$. As shown in the last section, there is a large room to adjust the value of $\mathscr{A}_t/\mathscr{A}_s$, even after the back-reactions are taken into account, which leads to the constraints of Eq.(2.32), from which we find that

$$\left(3 - 2\sqrt{2}\right)^2 \lesssim \frac{\mathscr{A}_t}{\mathscr{A}_s} \lesssim \left(3 + 2\sqrt{2}\right)^2. \tag{3.6}$$

In Fig. 3 and Fig. 4, we display four examples of the modified factor $\mathscr{A}_n$ for different sets of parameters $b_1, b_2,\ \epsilon_*$. It is shown clearly that the constraint for the modified factor of Eq.(2.28) can be easily realized by properly choosing the values of b_1, b_2, and ϵ_*.

It is worthwhile to emphasize that even though with the constraints on $\mathscr{A}_t/\mathscr{A}_s$ of Eq.(3.6), the quantum gravitational effects still provide a viable mechanism to reconcile the tension between some inflation models and the Planck2015 observational data. To illustrate this clearly, let us take a look at the simplest inflation model with a power-law potential $V(\phi) = \lambda_p\phi^p$ as an example. When the quantum gravitational effects are taken into account, as shown in Fig. 5, in which we take $\mathscr{A}_t/\mathscr{A}_s$ to be in the range $(0.48, 1.2)$, which is well within the constraints of Eq.(2.32), the inflation model with a quadratic potential now can be perfectly consistent with Planck 2015 data.

IV. CONCLUSIONS

The uniform asymptotic approximation method provides a powerful, systematically improvable, and error controlled approach to construct analytical solutions of inflationary perturbations. It has been applied to inflationary models in various situations, in which the traditional methods, such as WKB and Green functions, either are not applicable or produce large errors [11]. These include models with nonlinear dispersion relations [14, 16], k-inflation [17], and holonomy and inverse-volume corrections from LQC [18].

In this paper, we have systematically generalized our previous studies of quantum gravitational effects with the nonlinear dispersion relation (1.2) from the first-order approximations [14] to the third-order with any number and order of turning-points. The upper bounds of errors to the third-order approximations are $\leq 0.15\%$ [16], which are accurate enough for the current and forthcoming experiments [19].

To our goals, we have first derived the analytic approximate solutions of perturbations associated with different turning points to any order of approximations, and then matched them together to the third-order. With the matched solutions, we have been able to calculate explicitly the primordial tensor and scalar perturbation spectra, which represents the most accurate results in the literature, as far as we know. From these expressions, we have also derived several features of the power spectra due to quantum gravitational effects that may be observationally interesting.

After deriving explicitly the power spectra of the tensor and scalar perturbations up to the third-order approximation, we have investigated the constraints due to the back-reactions of quantum gravitational effects [20–22]. This is very important, in order to make sure that these effects will not make inflation end in a very early period, and the problems, such as horizon, flatness and monopole, are still solved. With a very conservative assumption about the energy scale M_* of the underlying theory of quantum gravity, we have found the bounds on the amplitudes of the power spectra, which are given explicitly by Eq.(3.6). Even with these severe constraints, we have found the tensions between certain inflationary models and observations can be reconciled easily, after quantum gravitational effects are taken into account. These include the chaotic model with a quadratic potential.

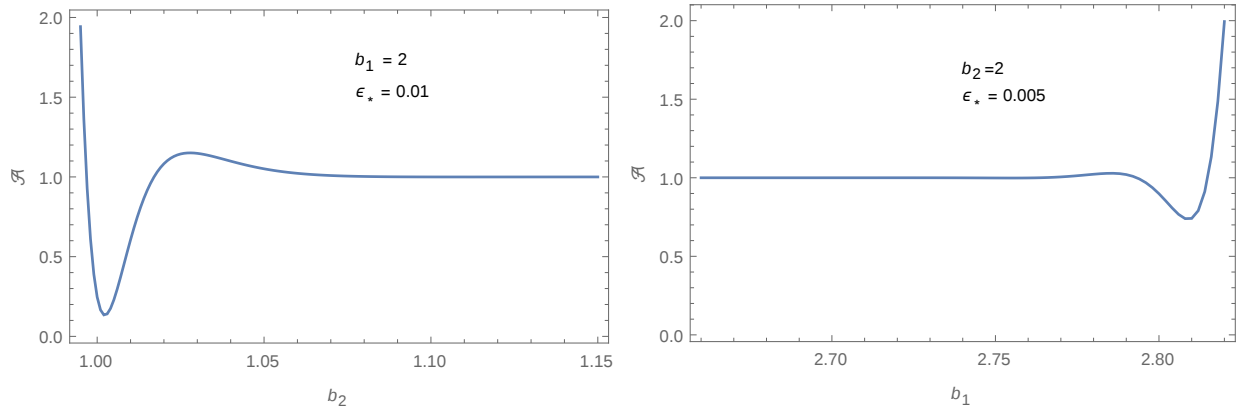

FIG. 3. The modified factor $\mathscr{A}$ for two different sets of parameters with $\nu = 3/2$. Left panel: the modified factor $\mathscr{A}$ vs b_2 with b_1 and ϵ_* fixed. Right panel: the modified factor $\mathscr{A}$ vs b_1 with b_2 and ϵ_* fixed.

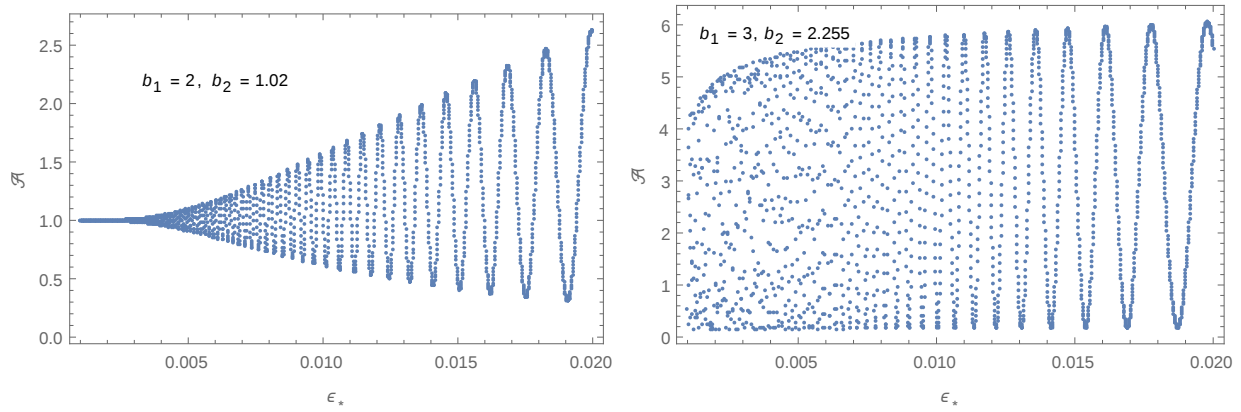

FIG. 4. The dependence of the modified factor $\mathscr{A}$ on ϵ_* for two different sets of parameters (b_1, b_2) but all with $\nu = 3/2$. (i) Left panel: the modified factor $\mathscr{A}$ vs ϵ_* with $b_1 = 2$ and $b_2 = 1.02$. In this case, for the range of ϵ_* we considered in the figure, the function $\lambda^2\hat{g}(y)$ has one single real and two complex turning points, which corresponds to Cases (c) and (d) in Fig. 2. When ϵ_* approaches to zero, the function $\lambda^2\hat{g}(y)$ gradually changes from Case (c) to Case (d), and the factor $\mathscr{A}$ approaches to one, as expected. (ii) Right panel: the modified factor $\mathscr{A}$ vs ϵ_* with $b_1 = 3$ and $b_2 = 2.255$. The values of the parameters chosen in this case correspond to the case in which the turning points y_1 and y_2 are real and very close to each other, i.e., $|y_1/y_2 - 1| \ll 1$, so that the modified factor $\mathscr{A} \simeq 3 + 2\sqrt{2}\cos 2\mathfrak{B}$.

Finally, we would like to note that, although we have studied the quantum gravitational effects specified by the nonlinear dispersion relation (1.2), in which the equation of motion could have three turning points, we would like to emphasize that the method and results presented in this paper can be easily extended to other cases. In particular, the method is equally well applicable to non-slow-roll inflationary models.

ACKNOWLEDGEMENTS

Part of the work was carried out when A.W. was visiting the State University of Rio de Janeiro (UERJ), Brazil. A.W. would like to express his gratitude to UERJ for hospitality. This work is supported in part by Ciência Sem Fronteiras, No. 004/2013 - DRI/CAPES, Brazil (A.W.); Chinese NSFC No. 11375153 (A.W.), No. 11173021 (A.W.), No. 11047008 (T.Z.), No. 11105120 (T.Z.), and No. 11205133 (T.Z.).

Appendix A: The uniform asymptotic approximation

In this appendix, we provide the novel ideas of the uniform asymptotic approximation with high-order approximations. The approximation scheme presented here provides a systematic and powerful approach to the second-order ordinary differential equation with various turning points, at which the WKB approximation becomes invalid. To make our formulas as much applicable as possible, in this appendix we shall present the development in a very general manner, so that we could easily extend the results to other circumstances.

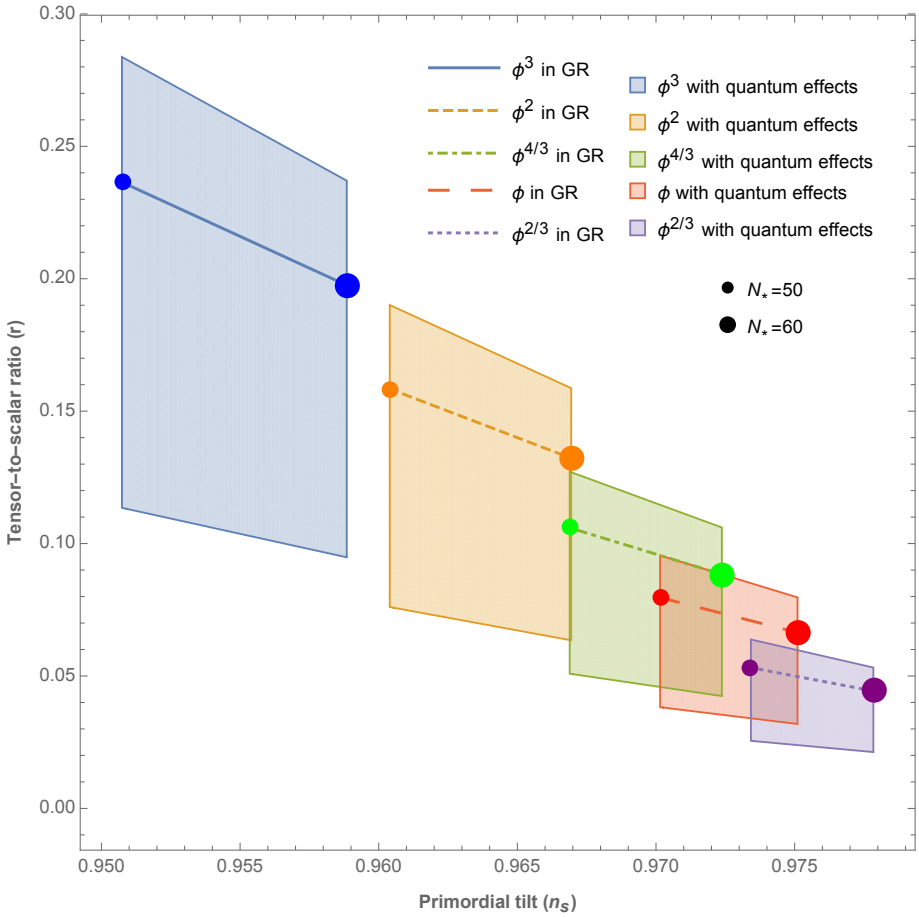

FIG. 5. Theoretical predictions for the inflationary models with the potential $V(\phi) = \lambda_p \phi^p$ after quantum gravitational effects are taken into account. In this figure, we take the ratio $\mathscr{A}_t/\mathscr{A}_s$ to be in the range $(0.48, 1.2)$, which is well within the constraints Eq.(2.32), obtained after the back-reactions are taken into account [20–22]. The upper limit of Planck2015 data is $r \leq 0.11$ at 95% C.L. The shaded quadrangle regions are the theoretical allowed regions of the parameters r and n_s for a given p. In the case $p = 2$ one can see that r can be as small as 0.07. As mentioned in the content, it can be even smaller for different choices of ϵ_* [26].

1. Equation of the Mode Function and Liouville Transformation

Our starting point is to consider the following second-order differential equation [23, 24],

$$\frac{d^2\mu_k(y)}{dy^2} = \Big[\lambda^2\hat{g}(y) + q(y)\Big]\mu_k(y), \tag{A.1}$$

where λ^2 is supposed to be a large positive parameter, and the functions $\lambda^2\hat{g}(y)$ and $q(y)$ will be determined by the analysis of the error bounds given below, so that the associated errors will be minimized. In general, $\lambda^2\hat{g}(y)$ and $q(y)$ could have poles or zeros in the interval of our interest. We also called the zeros of $\lambda^2\hat{g}(y)$ as turning points of the equation (A.1). From the theory of the second-order differential equation, the uniform asymptotic solution of $\mu_k(y)$ depends on the behavior of the functions $\lambda^2\hat{g}(y)$ and $q(y)$ around their poles (singularities) and zeros (turning points). Note that in this paper, we also use the notation $g(y) = \lambda^2\hat{g}(y)$, and in practice, when we turn to the final results, we may set $\lambda = 1$ for simplification.

To proceed further, let us introduce the Liouville transformation with two new variable $U(\xi)$ and $\xi(y)$ [23, 24],

$$U(\xi) = \chi^{1/4}\mu_k(y), \quad \chi = \xi'^2 = \frac{|\hat{g}(y)|}{f^{(1)}(\xi)^2}, \tag{A.2}$$

where $\xi' = d\xi/dy$, and

$$f(\xi) = \int \sqrt{|\hat{g}(y)|}dy, \quad f^{(1)}(\xi) = \frac{df(\xi)}{d\xi}. \tag{A.3}$$

Note that χ must be regular and not vanish in the intervals of interest. Consequently, the function $f(\xi)$ must be chosen so that $f^{(1)}(\xi)$ has zeros and singularities of the same type as those of $\hat{g}(y)$. As shown below, such requirements play an essential role in determining the approximate solutions. In terms of $U(\xi)$ and $\xi(y)$, Eq.(2.3)

is brought into the form,

$$\frac{d^2U(\xi)}{d\xi^2} = \Big[\pm\lambda^2 f^{(1)}(\xi)^2 + \psi(\xi)\Big]U(\xi), \quad \text{(A.4)}$$

where

$$\psi(\xi) = \frac{q(y)}{\chi} - \chi^{-3/4}\frac{d^2(\chi^{-1/4})}{dy^2}. \quad \text{(A.5)}$$

Here $\pm$ correspond to $\hat{g}(y) > 0$ and $\hat{g}(y) < 0$, respectively, and $\chi' \equiv d\chi/dy$. Considering $\psi(\xi) = 0$ as the first-order approximation, one must choose $f^{(1)}(\xi)^2$ so that: (a) the first-order approximation is as close to the exact solution as possible, and (b) the resulting equation can be solved explicitly (in terms of some known special functions). Clearly, such a choice sensitively depends on the behavior of the functions $\lambda^2\hat{g}(y)$ and $q(y)$ near the poles and zeros. Therefore, in the following let us first consider solutions near poles.

2. Liouville-Green approximations near poles

a. *Liouville-Green approximate solutions and their error bounds*

In most of physical systems, the regions of physical interest are in general in the intervals between two poles or on one side of them. In this section, let us assume that the functions $\lambda^2\hat{g}(y)$ and $q(y)$ have two poles, one is located at $y = 0^+$ and another is at $y = +\infty$. In addition, we assume $\hat{g}(y) > 0$ near $y = 0^+$ and $\hat{g}(y) < 0$ when $y \to +\infty$. Except the regions near the zeros of $\lambda^2\hat{g}(y)$, the functions $\lambda^2\hat{g}(y)$ and $q(y)$ are usually well-defined in their neighborhoods of poles. With this property, we can choose

$$f^{(1)}(\xi)^2 = \text{const.} \quad \text{(A.6)}$$

Without loss of generality, we can always set this constant to one. Then, from Eq. (A.2) we find

$$\xi(y) = \int \sqrt{\pm\hat{g}(y)}dy, \quad \text{(A.7)}$$

here "+" ("-") corresponds to $\hat{g}(y) > 0$ and $\hat{g}(y) < 0$ respectively, and the equation of motion (A.4) takes the form

$$\frac{d^2U(\xi)}{d\xi^2} = \left[\pm\lambda^2 + \psi(\xi)\right]U(\xi). \quad \text{(A.8)}$$

Let us first consider the approximate solution near the pole $y = 0^+$. In this case, we choose $\xi(y)$ as a monotone increasing function of y, thus we find

$$\xi(y) = \int_{y_i}^{y} \sqrt{\hat{g}(y')}dy', \quad \text{(A.9)}$$

where y_i is an irrelevant reference point near $y = 0^+$. Then, the equation of motion now reads

$$\frac{d^2U(\xi)}{d\xi^2} = \left[\lambda^2 + \psi(\xi)\right]U(\xi). \quad \text{(A.10)}$$

To the first-order approximation, that is, neglecting the $\psi(\xi)$ term in Eq. (A.10), the approximate solution takes the form $e^{\pm\lambda\xi}$. Then, the solution of Eq. (A.10) with error terms can be constructed as

$$U^+ = c_+e^{\lambda\xi}(1+\epsilon_1^+) + d_+e^{-\lambda\xi}(1+\epsilon_2^+), \quad \text{(A.11)}$$

where c_+, d_+ are integration constants, and ϵ_1^+ and ϵ_2^+ represent the errors of the approximate solution, which are bounded by

$$|\epsilon_1^+|, \ \frac{|d\epsilon_1^+/dy|}{2|\hat{g}|^{1/2}} \le \exp\left(\frac{1}{2}\mathscr{V}_{0,y}(\mathscr{F})\right) - 1,$$
$$|\epsilon_2^+|, \frac{|d\epsilon_2^+/dy|}{2|\hat{g}|^{1/2}} \le \exp\left(\frac{1}{2}\mathscr{V}_{y,+\infty}(\mathscr{F})\right) - 1. \quad \text{(A.12)}$$

The derivation of the error bounds can be found in [14, 23]. Here $\mathscr{F}(y)$ represents the associated error control function of the approximate solution, which is given by

$$\mathscr{F}(y) = \int |\psi(v)|dv = \int \left[\frac{1}{|g|^{1/4}}\frac{d^2}{dy^2}\left(\frac{1}{|g|^{1/4}}\right) - \frac{q}{|g|^{1/2}}\right]dy, \quad \text{(A.13)}$$

and $\mathscr{V}_{x_1,x_2}(\mathscr{F})$ is the total variation of the function $\mathscr{F}(y)$. Accordingly, the mode function $\mu_k(y)$ is given by the Liouville-Green (LG) solution

$$\mu_k^+(y) = \frac{c_+}{\hat{g}(y)^{1/4}}e^{\lambda\int_{y_i}^{y}\sqrt{\hat{g}(y')}dy'}(1+\epsilon_1^+) + \frac{d_+}{\hat{g}(y)^{1/4}}e^{-\lambda\int_{y_i}^{y}\sqrt{\hat{g}(y')}dy'}(1+\epsilon_2^+). \quad \text{(A.14)}$$

Similarly, near the pole $y = +\infty$, we still choose $\xi(y)$ as a monotone increasing function of y. So we have

$$\xi(y) = \int_{y_e}^{y}\sqrt{-\hat{g}(y')}dy', \quad \text{(A.15)}$$

where y_e is an irrelevant reference point near $y = +\infty$. Then Eq. (A.8) has the form,

$$\frac{d^2U(\xi)}{d\xi^2} = \left[-\lambda^2 + \psi(\xi)\right]U(\xi). \quad \text{(A.16)}$$

Ignoring the term $\psi(\xi)$ as the first-order approximation, the solution of the above equation now takes the form $\sim e^{\pm i\lambda\xi}$. Thus, the solution of Eq. (A.10) with the error terms near the pole $y \to \infty$ can be constructed as

$$U^- = c_-e^{i\lambda\xi}(1+\epsilon_1^-) + d_-e^{-i\lambda\xi}(1+\epsilon_2^-), \quad \text{(A.17)}$$

where c_-, d_- are other two integration constants, and ϵ_1^- and ϵ_2^- represent the associated errors of the approximation, and are bounded by

$$|\epsilon_1^-|, \ \frac{|d\epsilon_1^-/dy|}{|g|^{1/2}} \le \exp\left(\mathscr{V}_{y,+\infty}(\mathscr{F})\right) - 1, \quad \text{(A.18)}$$

$$|\epsilon_2^-|, \ \frac{|d\epsilon_2^-/dy|}{|g|^{1/2}} \le \exp\left(\mathscr{V}_{0,y}(\mathscr{F})\right) - 1. \quad \text{(A.19)}$$

Then the mode function $\mu_k^-(y)$ takes the form

$$\mu_k^-(y) = \frac{c_-}{(-\hat{g}(y))^{1/4}} e^{i\lambda \int_{y_e}^{y} \sqrt{-\hat{g}(y')}dy'}(1+\epsilon_1^-) + \frac{d_-}{(-\hat{g}(y))^{1/4}} e^{-i\lambda \int_{y_e}^{y} \sqrt{-\hat{g}(y')}dy'}(1+\epsilon_2^-). \tag{A.20}$$

b. Convergence of error control function near poles

The LG approximation is meaningful only when the following two conditions hold. First, in the interval of interest, one has to require that $|q(y)|$ is smaller than $\lambda^2\hat{g}(y)$ near both of the two poles. The second condition states that the associated error control function $\mathscr{F}(y)$ must be convergent near these poles. These two conditions provide guidelines for how to determine the splitting of $\lambda^2\hat{g}(y) + q(y)$.

Let us first consider the region near the pole $y = 0^+$, in which the function $\lambda^2\hat{g}(y)$ and $q(y)$ are expanded in the form

$$\lambda^2\hat{g}(y) = \frac{1}{y^i}\sum_{s=0}^{\infty} g_s y^s,\ q(y) = \frac{1}{y^j}\sum_{s=0}^{\infty} q_s y^s. \tag{A.21}$$

Note that in writing out the above expressions we have assumed that $\lambda^2\hat{g}(y)$ has a pole of order i and $q(y)$ has a pole of order j at $y = 0^+$. Substituting the above expansions into the integrand of the error control function in Eq. (A.13), we find

$$\frac{1}{\hat{g}^{1/4}}\frac{d^2}{dy^2}\left(\frac{1}{\hat{g}^{1/4}}\right) - \frac{q}{\hat{g}^{1/2}} = \frac{5}{16}\frac{\hat{g}'^2}{\hat{g}^{5/2}} - \frac{1}{4}\frac{\hat{g}''}{\hat{g}^{3/2}} - \frac{q}{\hat{g}^{1/2}}, \tag{A.22}$$

where

$$\begin{aligned} \frac{5}{16}\frac{\hat{g}'^2}{\hat{g}^{5/2}} &\simeq \frac{5}{16} y^{\frac{i}{2}-2}\left[4 g_0^{-1/2} + \mathcal{O}(y)\right], \\ -\frac{1}{4}\frac{\hat{g}''}{\hat{g}^{3/2}} &\simeq -\frac{1}{4} y^{\frac{i}{2}-2}\left[6 g_0^{-1/2} + \mathcal{O}(y)\right], \\ -\frac{q}{\hat{g}^{1/2}} &\simeq -y^{\frac{i}{2}-j}\left[q_0 g_0^{-1/2} + \mathcal{O}(y)\right]. \end{aligned} \tag{A.23}$$

With the above expansions, now let us discuss the convergence of the error control function $\mathscr{F}(y)$ by considering the following different cases.

- $i > 2$. In this case, the error control function $\mathscr{F}(y)$ is convergent only if $j < \frac{i}{2} + 1$, i.e.,

$$i > 2, \quad j < \frac{i}{2} + 1. \tag{A.24}$$

- $i = 2$. In this case, one also requires $j = 2$ and the error control function $\mathscr{F}(y)$ reads

$$\frac{5}{16}\frac{\hat{g}'^2}{\hat{g}^{5/2}} - \frac{1}{4}\frac{\hat{g}''}{\hat{g}^{3/2}} - \frac{q}{\hat{g}^{1/2}} \sim -g_0^{1/2}\left(\frac{1}{4} + q_0\right) y^{-1} + \mathcal{O}(y^0), \tag{A.25}$$

which yields

$$i = 2, \ \ j = 2, \ \ q_0 = -\frac{1}{4}. \tag{A.26}$$

- $i < 2$. In this case, the error control function $\mathscr{F}(y)$ can not be convergent for any choices of g_s and q_s.

Let us now turn to the pole $y = +\infty$. Assuming that $\hat{g}(y)$ and $q(y)$ have a pole of order i and j, respectively, we find that they can be expanded in the form,

$$g(y) = y^i\sum_{s=0}^{\infty}\bar{g}_s y^{-s},\ q(y) = y^j\sum_{s=0}^{\infty}\bar{q}_s y^{-s}, \tag{A.27}$$

where $\bar{g}_s$ and $\bar{q}_s$ are other sets of constants. Substituting the above expansions into the integrand of the error control function $\mathscr{F}(y)$ in Eq. (A.13), we find that

$$\frac{1}{|g|^{1/4}}\frac{d^2}{dy^2}\left(\frac{1}{|g|^{1/4}}\right) - \frac{q}{|g|^{1/2}} = y^{-2-i/2}\sum_{s=0}^{+\infty} c_s^{(1)} y^{-s} + y^{j-i/2}\sum_{s=0}^{+\infty} c_s^{(2)} y^{-s}, \tag{A.28}$$

where the coefficients $c_s^{(1)}$ and $c_s^{(2)}$ are functions of $\bar{q}_s$ and $\bar{g}_s$. Then, the convergence of $\mathscr{F}(y)$ requires

$$i > -2, \quad j < \frac{i}{2} - 1. \tag{A.29}$$

The validity of the uniform asymptotic approximation is very sensitive to the types of the poles of the function $\lambda^2\hat{g}(y)$. For the sake of further applications of the approximations, let us summarize the main conditions of the validity of the uniform asymptotic approximation as follows:

- $|q(y)| < |\lambda^2\hat{g}(y)|$ near both poles;
- at the pole $y = 0^+$, the function $\lambda^2\hat{g}(y)$ must be of order $i \geq 2$;
  - for $i > 2$, one has to choose $j < \frac{i}{2} + 1$;
  - for $i = 2$, one has to choose $q_0 = -1/4$ and $j = 2$;
- at the pole $y = +\infty$, the functions $\lambda^2\hat{g}(y)$ and $q(y)$ must chosen so that $i > -2$ and $j < i/2 - 1$.

Note that in the above i denotes the order of poles of the function $\lambda^2\hat{g}(y)$ and j denotes the order of the poles of the function $q(y)$. The physically interesting region lies in the range $y \in (0, +\infty)$, which may contain various turning points. Now, let us turn to the approximation solutions near turning points.

3. Approximate solution near the single turning point y_0

We first consider the single turning point at $y = y_0$ for the function $\lambda^2\hat{g}(y)$. Then, the function $\hat{g}(y)$ can be written in the form

$$\hat{g}(y) = p(y)(y - y_0), \tag{A.30}$$

where $p(y)$ is a regular function with $p(y_0) \neq 0$ and we also assume $p(y) < 0$ [4]. In order to perform the uniform asymptotic approximation, we assume that $|q(y)|$ *is small in comparison with* $|\lambda^2\hat{g}(y)|$*, except in the neighborhood of* y_0*, in which it must be smaller than* $\left|\lambda^2\hat{g}(y)(y-y_0)^{-1}\right|$ [14]. As we already mentioned previously, one has to choose $f^{(1)}(\xi)^2$ so that it has the same type of zeros or singularities as $\hat{g}(y)$. Thus, around the single turning point y_0, one can introduce a monotonically increasing or decreasing function ξ via the relation,

$$f^{(1)}(\xi)^2 = \pm\xi, \tag{A.31}$$

where $\xi(y_0) = 0$, and $\pm$ correspond to $\xi(y) > 0$ and $\xi(y) < 0$, respectively. Without loss of the generality, we can choose ξ to have the same sign as $\hat{g}(y)$, and thus ξ is a monotone decreasing function around $y = y_0$. Combining Eqs.(A.2) and (A.31), we find

$$\xi = \begin{cases} -\left(\frac{3}{2}\int_{y_0}^{y}\sqrt{-\hat{g}(y')}dy'\right)^{2/3}, & y \geq y_0, \\ \left(-\frac{3}{2}\int_{y_0}^{y}\sqrt{\hat{g}(y')}dy'\right)^{2/3}, & y \leq y_0, \end{cases} \tag{A.32}$$

and that Eq.(A.4) now reads

$$\frac{d^2U}{d\xi^2} = \Big(\lambda^2\xi + \psi(\xi)\Big)U. \tag{A.33}$$

Neglecting the $\psi(\xi)$ term, we find that the above equation has the approximate analytical solution in terms of Airy type functions

$$U(\xi) \sim \mathrm{Ai}(\lambda^{2/3}\xi) \quad \text{or} \quad \mathrm{Bi}(\lambda^{2/3}\xi). \tag{A.34}$$

Then, the solution of Eq. (A.33) can be casted into the form

$$U(\xi) = \alpha_0\Big(\mathrm{Ai}(\lambda^{2/3}\xi) + \epsilon_3^{(1)}\Big) + \beta_0\Big(\mathrm{Bi}(\lambda^{2/3}\xi) + \epsilon_4^{(1)}\Big), \tag{A.35}$$

where $\mathrm{Ai}(\xi)$ and $\mathrm{Bi}(\xi)$ are the Airy functions, α_0 and β_0 are two integration constants, and $\epsilon_3^{(1)}$ and $\epsilon_4^{(1)}$ denote the errors of the first-order approximation, which are bounded by [14, 23]

$$\frac{|\epsilon_3|}{M(\xi)},\ \frac{|\partial\epsilon_3/\partial\xi|}{N(\xi)} \leq \frac{E^{-1}(\xi)}{\lambda_0}\Big\{\exp\Big(\lambda\mathscr{V}_{\xi,a_3}(\mathscr{H})\Big) - 1\Big\},$$

$$\frac{|\epsilon_4|}{M(\xi)},\ \frac{|\partial\epsilon_4/\partial\xi|}{N(\xi)} \leq \frac{E(\xi)}{\lambda_0}\Big\{\exp\Big(\lambda\mathscr{V}_{a_4,\xi}(\mathscr{H})\Big) - 1\Big\}, \tag{A.36}$$

where the auxiliary functions $M(\xi)$, $E(\xi)$, and constant λ_0 are given in [14]. $\mathscr{V}_{x_1,x_2}(F)$ is the supremum of the function $F(x)$ in the range (x_1, x_2). a_3 and a_4 are, respectively, the upper and lower limit of the variable ξ. And $\mathscr{H}$ is the associated error control function, which is defined as

$$\mathscr{H}(\xi) = \int_0^{\xi} |v|^{-1/2}\psi(v)dv. \tag{A.37}$$

Then, the mode function is given by,

$$\mu_k(y) = \alpha_0\left(\frac{\xi(y)}{\hat{g}(y)}\right)^{1/4}\Big(\mathrm{Ai}(\lambda^{2/3}\xi) + \epsilon_3^{(1)}\Big) + \beta_0\left(\frac{\xi(y)}{\hat{g}(y)}\right)^{1/4}\Big(\mathrm{Bi}(\lambda^{2/3}\xi) + \epsilon_4^{(1)}\Big). \tag{A.38}$$

Now let us turn to extend the above first-order approximation to high orders. For this purpose, following Olver [16, 23], we assume that the exact solution of $U(\xi)$ takes the form (for the branches of $\mathrm{Ai}(\lambda^{2/3}\xi)$),

$$U(\lambda,\xi) = A(\lambda,\xi)\mathrm{Ai}(\lambda^{2/3}\xi) + \lambda^{-4/3}B(\lambda,\xi)\mathrm{Ai}'(\lambda^{2/3}\xi), \tag{A.39}$$

where for the first-order approximation we have $A(\lambda,\xi) = 1$ and $B(\lambda,\xi) = 0$. Substituting the above expression into the equation of motion (A.33) and equating the coefficients of $\mathrm{Ai}(x)$ and $\mathrm{Ai}'(x)$, we have

$$\begin{aligned} 2\lambda^2 A' + B'' - \psi B = 0, \\ A'' + B + 2\xi B' - \psi A = 0. \end{aligned} \tag{A.40}$$

These equations are satisfied by the formal expansions of the forms,

$$\begin{aligned} A(\lambda,\xi) &= \sum_{s=0}^{+\infty}\lambda^{-2s}A_s(\xi), \\ B(\lambda,\xi) &= \sum_{s=0}^{+\infty}\lambda^{-2s}B_s(\xi), \end{aligned} \tag{A.41}$$

so that

$$\begin{aligned} 2A'_{s+1} + B''_s - \psi B_s = 0, \\ A''_s + B_s + 2\xi B'_s - \psi A_s = 0. \end{aligned} \tag{A.42}$$

Integration of the above two equations yields,

$$\begin{aligned} A_0(\xi) &= 1, \\ B_s &= \frac{\pm 1}{2(\pm\xi)^{1/2}}\int_0^{\xi}\{\psi(v)A_s(v) - A''_s(v)\}\frac{dv}{(\pm v)^{1/2}}, \\ A_{s+1}(\xi) &= -\frac{1}{2}B'_s(\xi) + \frac{1}{2}\int\psi(v)B_s(v)dv, \end{aligned}$$

[4] This assumption is set to be consistent with case we are going to apply in this paper.

(A.43)

where $\pm$ correspond to $\xi \geq 0$ and $\xi \leq 0$, respectively.

Similarly, for the branches $\mathrm{Bi}(\lambda^{2/3}\xi)$, we find

$$U(\lambda,\xi) = \hat{A}(\lambda,\xi)\mathrm{Bi}(\lambda^{2/3}\xi) + \lambda^{-4/3}\hat{B}(\lambda,\xi)\mathrm{Bi}'(\lambda^{2/3}\xi). \tag{A.44}$$

It is easy to check that $\hat{A}(\lambda,\xi)$ and $\hat{B}(\lambda,\xi)$ have the same expressions as those given in Eq.(A.43). Then, the approximate solution of $U(\xi)$ up to the $(2n)$-th order of the approximation can be expressed as [16, 23]

$$\begin{aligned} U(\lambda,\xi) = \alpha_0 \Bigg[& \mathrm{Ai}(\lambda^{2/3}\xi) \sum_{s=0}^{n} \frac{A_s(\xi)}{\lambda^{2s}} \\ & + \frac{\mathrm{Ai}'(\lambda^{2/3}\xi)}{\lambda^{4/3}} \sum_{s=0}^{n-1} \frac{B_s(\xi)}{\lambda^{2s}} + \epsilon_3^{(2n+1)} \Bigg] \\ + \beta_0 \Bigg[& \mathrm{Bi}(\lambda^{2/3}\xi) \sum_{s=0}^{n} \frac{A_s(\xi)}{\lambda^{2s}} \\ & + \frac{\mathrm{Bi}'(\lambda^{2/3}\xi)}{\lambda^{4/3}} \sum_{s=0}^{n-1} \frac{B_s(\xi)}{\lambda^{2s}} + \epsilon_4^{(2n+1)} \Bigg], \end{aligned} \tag{A.45}$$

where the error bounds $\epsilon_3^{(2n+1)}$ and $\epsilon_4^{(2n+1)}$ for the $(2n)$-th order are given by

$$\begin{aligned} & \frac{\epsilon_3^{(2n+1)}}{M(\lambda^{2/3}\xi)}, \quad \frac{\partial\epsilon_3^{(2n+1)}/\partial\xi}{\lambda^{2/3}N(\lambda^{2/3}\xi)} \\ & \quad \leq 2E^{-1}(\lambda^{2/3}\xi)\exp\left\{\frac{2\kappa_0 \mathscr{V}_{\alpha,\xi}(|\xi^{1/2}|B_0)}{\lambda}\right\} \\ & \qquad \times \frac{\mathscr{V}_{\alpha,\xi}(|\xi^{1/2}|B_n)}{\lambda^{2n+1}}, \\ & \frac{\epsilon_4^{(2n+1)}}{M(\lambda^{2/3}\xi)}, \quad \frac{\partial\epsilon_4^{(2n+1)}/\partial\xi}{\lambda^{2/3}N(\lambda^{2/3}\xi)} \\ & \quad \leq 2E(\lambda^{2/3}\xi)\exp\left\{\frac{2\kappa_0 \mathscr{V}_{\xi,\beta}(|\xi^{1/2}|B_0)}{\lambda}\right\} \\ & \qquad \times \frac{\mathscr{V}_{\xi,\beta}(|\xi^{1/2}|B_n)}{\lambda^{2n+1}}. \end{aligned} \tag{A.46}$$

4. Approximate solution near the turning points y_1 and y_2

Except single turning points, the uniform asymptotic approximation can be also applied to other types of turning points, like high-order turing or multi-turning points. In this subsection, we shall consider a pair of turning points, y_1 and y_2, which could be both single and real, coalescent, or complex conjugate. In the neighborhoods of this type of turning points, we have

$$\hat{g}(y) = p(y)(y-y_1)(y-y_2), \tag{A.47}$$

where $p(y)$ is regular in the interval of interest, and $p(y_1) \neq 0$ and $p(y_2) \neq 0$. Without loss of the generality, here we assume that $p(y) < 0$ when $y < y_1$ and $y > y_2$ with $y_1 < y_2$. In general, we have three different cases depending on the nature of the two turning points y_1 and y_2,

- y_1 and y_2 are two distinct real roots of $\hat{g}(y)$, i.e., *two single and real turning points* [c.f. Case (a) in Fig. 2];
- $y_1 = y_2$, a double root of $\hat{g}(y)$, i.e., *a double turning point* [c.f. Case (b) in Fig. 2];
- y_1 and y_2 are two complex roots of $\hat{g}(y)$, i.e., *two complex conjugate turning points* [c.f. Cases (c) and (d) in Fig. 2]. Recall that the difference between Cases (c) and (d) is that for Case (d), the two complex roots are largely spaced in the imaginary axis.

In the uniform asymptotic approximation, we require the condition that *the function $|q(y)|$ be small compared with $|\lambda^2\hat{g}(y)|$, except in the neighborhoods of $y = y_1$ and $y = y_2$, in which it must be smaller than $|\lambda^2\hat{g}(y)(y-y_1)^{-1}(y-y_2)^{-1}|$* [14]. Following Olver [24], we shall adopt a method to treat all of the above cases together. The crucial point is to choose $f^{(1)}(\zeta)^2$ in the Liouville transformation (A.2) so that [5]

$$f^{(1)}(\zeta)^2 = |\zeta^2 - \zeta_0^2|, \tag{A.48}$$

where we choose ζ to be an increasing function of y, and with the conditions $\zeta(y_1) = -\zeta_0$ and $\zeta(y_2) = \zeta_0$. The quantity ζ_0^2 can be positive, zero, and negative, depending on whether $y_{1,2}$ are both real and different $y_1 \neq y_2$, or both real but equal $y_1 = y_2$, or $y_{1,2}$ are complex conjugate. Then, it can be shown that ζ_0^2 can be expressed as,

$$\zeta_0^2 = \frac{2}{\pi}\int_{y_1}^{y_2} \sqrt{\hat{g}(y)}dy. \tag{A.49}$$

Now let us turn to derive the relation between $\zeta(y)$ and y. We first consider the case where y_1 and y_2 are real and $y > y_2$, so that $\zeta(y) > \zeta_0$. Then, from Eq.(A.2) we find

$$\int_{\zeta_0}^{\zeta} \sqrt{v^2 - \zeta_0^2}dv = \int_{y_2}^{y} \sqrt{-\hat{g}(y')}dy', \tag{A.50}$$

which yields

$$\int_{y_2}^{y} \sqrt{-\hat{g}(y')}dy' = \frac{1}{2}\zeta\sqrt{\zeta^2 - \zeta_0^2} - \frac{\zeta_0^2}{2}\,\mathrm{arcosh}\left(\frac{\zeta}{\zeta_0}\right). \tag{A.51}$$

When $y < y_1$, we have $\zeta(y) < -\zeta_0$, then from Eq.(A.2) we find

$$\int_{-\zeta_0}^{\zeta} \sqrt{v^2 - \zeta_0^2}dv = \int_{y_1}^{y} \sqrt{-\hat{g}(y')}dy', \tag{A.52}$$

[5] Here we use ζ to denote the variable $\xi(y)$ in the Liouville transformation, for the purpose to distinguish with the variable $\xi(y)$ used for the y_0 case.

which yields

$$\int_{y_1}^{y}\sqrt{-\hat{g}(y')}dy'=\frac{1}{2}\zeta\sqrt{\zeta^2-\zeta_0^2}+\frac{\zeta_0^2}{2}\,\mathrm{arcosh}\left(-\frac{\zeta}{\zeta_0}\right). \tag{A.53}$$

When $y_1\le y\le y_2$, we have $-\zeta_0<\zeta(y)<\zeta_0$, and

$$\int_{-\zeta_0}^{\zeta}\sqrt{\zeta_0^2-v^2}dv=\int_{y_1}^{y}\sqrt{\hat{g}(y')}dy', \tag{A.54}$$

which yields

$$\int_{y_1}^{y}\sqrt{\hat{g}(y')}dy'=\frac{1}{2}\zeta\sqrt{\zeta^2-\zeta_0^2}+\frac{\zeta_0^2}{2}\arccos\left(-\frac{\zeta}{\zeta_0}\right). \tag{A.55}$$

Now let us turn to consider the case where y_1 and y_2 are complex conjugate. In this case ζ_0^2 is always negative, thus from Eq.(A.2) one finds

$$\int_0^{\zeta}\sqrt{\zeta^2-\zeta_0^2}d\zeta=\int_{\mathrm{Re}(y_1)}^{y}\sqrt{-\hat{g}(y')}dy', \tag{A.56}$$

which yields

$$\begin{aligned}&\int_{\mathrm{Re}(y_1)}^{y}\sqrt{-\hat{g}(y')}dy'\\&=\frac{1}{2}\zeta\sqrt{\zeta^2-\zeta_0^2}-\frac{\zeta_0^2}{2}\ln\left(\frac{\zeta+\sqrt{\zeta^2-\zeta_0^2}}{|\zeta_0|}\right).\end{aligned} \tag{A.57}$$

Then, with $f^{(1)}(\zeta)^2$ given by Eq.(A.48), Eq.(A.4) reduces to

$$\frac{d^2U}{d\zeta^2}=\left[\lambda^2\left(\zeta_0^2-\zeta^2\right)+\psi(\zeta)\right]U. \tag{A.58}$$

Neglecting the $\psi(\zeta)$ term, we find that the approximate solution can be expressed in terms of the parabolic cylinder functions $W(\frac{1}{2}\lambda\zeta_0^2,\pm\sqrt{2\lambda}\zeta)$, and is given by

$$\begin{aligned}U(\zeta)=\alpha_1&\left\{W\left(\frac{1}{2}\lambda\zeta_0^2,\sqrt{2\lambda}\zeta\right)+\epsilon_5^{(1)}\right\}\\&+\beta_1\left\{W\left(\frac{1}{2}\lambda\zeta_0^2,-\sqrt{2\lambda}\zeta\right)+\epsilon_6^{(1)}\right\},\end{aligned} \tag{A.59}$$

from which we find

$$\begin{aligned}\mu_k(y)=\alpha_1&\left(\frac{\zeta^2-\zeta_0^2}{-\hat{g}(y)}\right)^{\frac{1}{4}}\left[W\left(\frac{1}{2}\lambda\zeta_0^2,\sqrt{2\lambda}\zeta\right)+\epsilon_5^{(1)}\right]\\&+\beta_1\left(\frac{\zeta^2-\zeta_0^2}{-\hat{g}(y)}\right)^{\frac{1}{4}}\left[W\left(\frac{1}{2}\lambda\zeta_0^2,-\sqrt{2\lambda}\zeta\right)+\epsilon_6^{(1)}\right],\end{aligned} \tag{A.60}$$

where $\epsilon_5^{(1)}$ and $\epsilon_6^{(1)}$ are the errors of the corresponding first-order approximations, which are bounded by

$$\begin{aligned}&\frac{|\epsilon_5^{(1)}|}{M\left(\frac{1}{2}\lambda\zeta_0^2,\sqrt{2\lambda}\zeta\right)},\ \frac{|\partial\epsilon_5^{(1)}/\partial\zeta|}{\sqrt{2}N\left(\frac{1}{2}\lambda\zeta_0^2,\sqrt{2\lambda}\zeta\right)}\\&\le\frac{\kappa}{\lambda_0E\left(\frac{1}{2}\lambda\zeta_0^2,\sqrt{2\lambda}\zeta\right)}\left\{\exp\left(\lambda\mathscr{V}_{\zeta,a_5}(\mathscr{I})\right)-1\right\},\\&\frac{|\epsilon_6^{(1)}|}{M\left(\frac{1}{2}\lambda\zeta_0^2,\sqrt{2\lambda}\zeta\right)},\ \frac{|\partial\epsilon_6^{(1)}/\partial\zeta|}{\sqrt{2}N\left(\frac{1}{2}\lambda\zeta_0^2,\sqrt{2\lambda}\zeta\right)}\\&\le\frac{\kappa E\left(\frac{1}{2}\lambda\zeta_0^2,\sqrt{2\lambda}\zeta\right)}{\lambda}\left\{\exp\left(\lambda_0\mathscr{V}_{a_6,\zeta}(\mathscr{I})\right)-1\right\},\end{aligned} \tag{A.61}$$

where $M\left(\frac{1}{2}\lambda\zeta_0^2,\sqrt{2\lambda}\zeta\right)$, $N\left(\frac{1}{2}\lambda\zeta_0^2,\sqrt{2\lambda}\zeta\right)$, and $E\left(\frac{1}{2}\lambda\zeta_0^2,\sqrt{2\lambda}\zeta\right)$ are auxiliary functions of the parabolic cylinder functions which are given in [14], a_5 and a_6 denotes the upper and lower limit of the variable ζ respectively, and

$$\mathscr{I}(\zeta)\equiv\int\frac{\psi(\zeta)}{\sqrt{|\zeta^2-\zeta_0^2|}}dv, \tag{A.62}$$

is the associated error control function for the approximate solutions near y_1 and y_2.

Now we need to extend the above first-order approximate solution to high orders. Following Olver [24], we assume that the exact solution $U(\lambda,\zeta)$ takes the form (for the branch of $W(\frac{1}{2}\lambda\zeta_0^2,\sqrt{2\lambda}\zeta)$)

$$\begin{aligned}U(\lambda,\zeta)=C(\lambda,\zeta)&W\left(\frac{1}{2}\lambda\zeta_0^2,\sqrt{2\lambda}\zeta\right)\\&+\frac{\sqrt{2\lambda}}{\lambda^2}D(\lambda,\zeta)W'\left(\frac{1}{2}\lambda\zeta_0^2,\sqrt{2\lambda}\zeta\right),\end{aligned} \tag{A.63}$$

where

$$W'\left(\frac{1}{2}\lambda\zeta_0^2,\sqrt{2\lambda}\zeta\right)\equiv\frac{\partial W(\frac{1}{2}\lambda\zeta_0^2,\sqrt{2\lambda}\zeta)}{\partial(\sqrt{2\lambda}\zeta)}. \tag{A.64}$$

As a result, we find

$$W''\left(\frac{1}{2}\lambda\zeta_0^2,\sqrt{2\lambda}\zeta\right)=\frac{\lambda}{2}(\zeta_0^2-\zeta^2)W\left(\frac{1}{2}\lambda\zeta_0^2,\sqrt{2\lambda}\zeta\right). \tag{A.65}$$

For the first-order approximation we have $C(\lambda,\zeta)=1$ and $D(\lambda,\zeta)=0$. Substituting Eq.(A.71) into the equation of motion and then equating the coefficients of $W(\frac{1}{2}\lambda\zeta_0^2,\sqrt{2\lambda}\zeta)$ and $W'(\frac{1}{2}\lambda\zeta_0^2,\sqrt{2\lambda}\zeta)$, we obtain

$$\begin{aligned}2\lambda^2C'+D''-\psi D=0,\\C''-2\zeta D-2(\zeta^2-\zeta_0^2)D'-\psi C=0.\end{aligned} \tag{A.66}$$

Expanding the functions C and D as

$$\begin{aligned}C(\lambda,\zeta)=\sum_{s=0}^{+\infty}\lambda^{-2s}C_s(\zeta),\\D(\lambda,\zeta)=\sum_{s=0}^{+\infty}\lambda^{-2s}D_s(\zeta),\end{aligned} \tag{A.67}$$

we find

$$2C'_{s+1} + D''_s - \psi D_s = 0,$$
$$C''_s - 2\zeta D_s - 2(\zeta^2 - \zeta_0^2)D'_s - \psi C_s = 0. \quad \text{(A.68)}$$

Integration of the above two equations leads to,

$$C_0(\zeta) = 1,$$
$$D_s(\zeta) = \begin{cases} \frac{1}{2\sqrt{\zeta^2-\zeta_0^2}} \int_{\zeta_0}^{\zeta} \frac{C''_s(v)-\psi(v)C_s(v)}{\sqrt{v^2-\zeta_0^2}} dv & |\zeta| \geq |\zeta_0|, \\ \frac{-1}{2\sqrt{\zeta_0^2-\zeta^2}} \int_{\zeta_0}^{\zeta} \frac{C''_s(v)-\psi(v)C_s(v)}{\sqrt{\zeta_0^2-v^2}} dv & |\zeta| \leq |\zeta_0|, \end{cases}$$
$$C_{s+1}(\zeta) = -\frac{1}{2}D'_s(\zeta) + \frac{1}{2}\int^{\zeta} \psi(v)D_s(v)dv. \quad \text{(A.69)}$$

Similarly, for the branch $W(\frac{1}{2}\lambda\zeta_0^2, -\sqrt{2\lambda}\zeta)$, we find

$$U(\zeta) = \hat{C}(\lambda,\zeta)W\left(\frac{1}{2}\lambda\zeta_0^2, -\sqrt{2\lambda}\zeta\right) - \frac{\sqrt{2\lambda}}{\lambda^2}\hat{D}(\lambda,\zeta)W'\left(\frac{1}{2}\lambda\zeta_0^2, -\sqrt{2\lambda}\zeta\right). \quad \text{(A.70)}$$

Here $\hat{C}(\lambda,\zeta)$ and $\hat{D}(\lambda,\zeta)$ have the same expressions as those given in Eq.(A.69). Then, the approximate solution $U(\zeta)$ up to the $(2n)$-th order can be expressed as

$$U(\zeta) = \alpha_1\left[W\left(\frac{1}{2}\lambda\zeta_0^2, \sqrt{2\lambda}\zeta\right)\sum_{s=0}^{n}\frac{C_s(\zeta)}{\lambda^{2s}} + \frac{\sqrt{2\lambda}W'\left(\frac{1}{2}\lambda\zeta_0^2, \sqrt{2\lambda}\zeta\right)}{\lambda^2}\sum_{s=0}^{n-1}\frac{D_s(\zeta)}{\lambda^{2s}} + \epsilon_5^{(2n+1)}\right]$$
$$+\beta_1\left[W\left(\frac{1}{2}\lambda\zeta_0^2, -\sqrt{2\lambda}\zeta\right)\sum_{s=0}^{n}\frac{C_s(\zeta)}{\lambda^{2s}} - \frac{\sqrt{2\lambda}W'\left(\frac{1}{2}\lambda\zeta_0^2, -\sqrt{2\lambda}\zeta\right)}{\lambda^2}\sum_{s=0}^{n-1}\frac{D_s(\zeta)}{\lambda^{2s}} + \epsilon_6^{(2n+1)}\right], \quad \text{(A.71)}$$

with

$$\frac{|\epsilon_5^{(2n+1)}|}{M(\frac{1}{2}\lambda\zeta_0^2, \sqrt{2\lambda}\zeta)}, \frac{|\partial\epsilon_5^{(2n+1)}/\partial\zeta|}{\sqrt{2\lambda}N(\frac{1}{2}\lambda\zeta_0^2, \sqrt{2\lambda}\zeta)} \leq \frac{\kappa\exp\left(\frac{\kappa_0}{\lambda}\mathscr{V}_{\zeta,a_5}(\sqrt{|\zeta^2-\zeta_0^2|}D_0)\right)}{E(\frac{1}{2}\lambda\zeta_0^2, \sqrt{2\lambda}\zeta)}\frac{\mathscr{V}_{\zeta,a_5}(\sqrt{|\zeta^2-\zeta_0^2|}D_n)}{\lambda^{2n+1}},$$
$$\frac{|\epsilon_6^{(2n+1)}|}{M(\frac{1}{2}\lambda\zeta_0^2, \sqrt{2\lambda}\zeta)}, \frac{|\partial\epsilon_6^{(2n+1)}/\partial\zeta|}{\sqrt{2\lambda}N(\frac{1}{2}\lambda\zeta_0^2, \sqrt{2\lambda}\zeta)} \leq \frac{\kappa\exp\left(\frac{\kappa_0}{\lambda}\mathscr{V}_{a_6,\zeta}(\sqrt{|\zeta^2-\zeta_0^2|}D_0))\right)}{E^{-1}(\frac{1}{2}\lambda\zeta_0^2, \sqrt{2\lambda}\zeta)}\frac{\mathscr{V}_{a_6,\zeta}(\sqrt{|\zeta^2-\zeta_0^2|}D_n)}{\lambda^{2n+1}}. \quad \text{(A.72)}$$

where $\epsilon_5^{(2n+1)}$ and $\epsilon_6^{(2n+1)}$ are errors of the $(2n)$-th order approximation.

Appendix B: Matching of the approximate solutions

1. Matching of the approximate solutions

Now we need to match the individual solutions obtained above together. The first step is to match the approximate solution associated with turning points y_1 and y_2 with the following initial condition,

$$\lim_{y\to+\infty}\mu_k(y) = \frac{1}{\sqrt{2\omega}}e^{-i\int\omega d\eta} \simeq \sqrt{\frac{1}{2\lambda k}}\frac{1}{(-\hat{g})^{1/4}}\exp\left(i\lambda\int_{y_i}^{y}\sqrt{-\hat{g}}dy\right). \quad \text{(B.1)}$$

However, the approximate solution involves so many high-order terms, which make the matching very complicated. In order to simplify it, let us study their behavior in the limit $y \to +\infty$. Let us first consider the $D_0(\zeta)$ term in Eq.(A.71), which is given by

$$D_0(\zeta) = -\frac{1}{2\sqrt{\zeta^2-\zeta_0^2}}\int_{\zeta_0}^{\zeta}\frac{\psi(v)}{\sqrt{v^2-\zeta_0^2}}dv$$
$$= -\frac{\mathscr{I}(\zeta)}{2\sqrt{\zeta^2-\zeta_0^2}}. \quad \text{(B.2)}$$

Note that in the above expression we had used $C_0(\zeta) = 1$, where $\mathscr{I}(\zeta)$ is the error control function associated with the approximate solution around y_1 and y_2, which behaves well around these two turning points. The integrand in the error control function can be expressed as

$$\frac{\psi(v)}{\sqrt{v^2-\zeta_0^2}} = \left[\frac{q}{\hat{g}} - \frac{5(\hat{g}')^2 - 4\hat{g}\hat{g}''}{16\hat{g}^3} + \frac{5\zeta_0^2}{4(v^2-\zeta_0^2)^3} + \frac{3}{4(v^2-\zeta_0^2)^2}\right]\sqrt{v^2-\zeta_0^2}, \quad \text{(B.3)}$$

and using $\sqrt{v^2-\zeta_0^2}dv = \sqrt{-\hat{g}}dy$, we find that

$$\mathscr{I}(\zeta) = \mathscr{F}(\zeta) + \int_{\zeta_0}^{\zeta}\left[\frac{5\zeta_0^2}{4(v^2-\zeta_0^2)^{5/2}} + \frac{3}{4(v^2-\zeta_0^2)^{3/2}}\right]dv, \quad \text{(B.4)}$$

where $\mathscr{F}(\zeta)$ is the associated error control function of the Liouville-Green (LG) approximate solution near the

pole $y=+\infty$ [14]. Obviously in the limit $y\to+\infty$, we have $\mathscr{I}(\zeta)\to\mathscr{F}(\zeta)$, which has been already proved to be convergent. As a result, we have

$$\lim_{y\to+\infty} D_0(\zeta)=-\frac{\mathscr{I}(+\infty)}{2\sqrt{\zeta^2-\zeta_0^2}}. \tag{B.5}$$

Then, let us turn to the next order, the term C_1, which is given by

$$C_1(\zeta)=-\frac{1}{2}D_0'(\zeta)+\frac{1}{2}\int_{\zeta_0}^{\zeta}\psi(v)D_0(v)dv. \tag{B.6}$$

In the limit $y\to+\infty$, $D_0'(\zeta)$ becomes negligible, and we find

$$\begin{aligned}\lim_{y\to+\infty} C_1(\zeta)&=-\frac{1}{2}\int_{\zeta_0}^{\zeta}\frac{\psi(v)}{\sqrt{v^2-\zeta_0^2}}\left[\frac{1}{2}\int_{\zeta_0}^{v}\frac{\psi(u)}{\sqrt{u^2-\zeta_0^2}}du\right]dv\\&=-\frac{1}{2}\left[\frac{\mathscr{I}(+\infty)}{2}\right]^2.\end{aligned} \tag{B.7}$$

In writing down the above expression we have used the formula

$$\begin{aligned}&n!\int_{\zeta_0}^{\zeta}f(\zeta_n)\int_{\zeta_0}^{\zeta_n}f(\zeta_{n-1})\cdots\int_{\zeta_0}^{\zeta_2}f(\zeta_1)d\zeta_1d\zeta_2\cdots d\zeta_n\\&\quad=\left[\int_{\zeta_0}^{\zeta}f(v)dv\right]^n.\end{aligned} \tag{B.8}$$

Thus, up to the third-order, we have

$$\begin{aligned}C(\lambda,\zeta)&=1-\frac{1}{2\lambda^2}\left[\frac{\mathscr{I}(+\infty)}{2}\right]^2+\mathcal{O}\left(\frac{1}{\lambda^3}\right),\\\frac{D(\lambda,\zeta)}{\lambda}&=-\frac{1}{\sqrt{\zeta^2-\zeta_0^2}}\frac{\mathscr{I}(+\infty)}{2\lambda}+\mathcal{O}\left(\frac{1}{\lambda^3}\right).\end{aligned} \tag{B.9}$$

Using the asymptotic forms of the parabolic cylinder functions presented in Appendix A, on the other hand, we find,

$$\begin{aligned}&\lim_{y\to+\infty}\mu_k(y)\\&=\left(\frac{-1}{\lambda\hat{g}}\right)^{\frac{1}{4}}\left\{(2j^2)^{1/4}\alpha_1\left(C\cos\mathfrak{D}-\frac{\bar{D}}{\lambda}\sin\mathfrak{D}\right)\right.\\&\qquad\left.+(2j^{-2})^{1/4}\beta_1\left(C\sin\mathfrak{D}+\frac{\bar{D}}{\lambda}\cos\mathfrak{D}\right)\right\},\end{aligned} \tag{B.10}$$

where $\bar{D}\equiv\sqrt{\zeta^2-\zeta_0^2}D$, $j=j(\sqrt{\lambda}\zeta_0)$, and

$$\begin{aligned}\mathfrak{D}&\equiv\frac{\lambda}{2}\zeta\sqrt{\zeta^2-\zeta_0^2}-\frac{\lambda}{2}\zeta_0^2\ln\left(\frac{\zeta+\sqrt{\zeta^2-\zeta_0^2}}{\zeta_0}\right)\\&\quad+\frac{\pi}{4}+\phi\left(\frac{\lambda}{2}\zeta_0^2\right)\\&=\lambda\int_{y_2}^{y}\sqrt{-\hat{g}(y')}dy'+\frac{\pi}{4}+\phi\left(\frac{\lambda}{2}\zeta_0^2\right).\end{aligned} \tag{B.11}$$

Here the function $\phi(x)$ is given by Eq.(C.6). Note that in order to get Eq.(B.10), we have ignored all the high order terms in the asymptotic expansions of the parabolic cylinder functions, as they all become negligible in the limit $y\to+\infty$. Now comparing the above solution with the initial condition, we obtain

$$\begin{aligned}\alpha_1&=\frac{\lambda^{-1/4}}{[2j^2(\sqrt{\lambda}\zeta_0)]^{1/4}}\frac{1}{\sqrt{2k}}\frac{e^{-iX}}{C+i\bar{D}/\lambda},\\\beta_1&=\frac{\lambda^{-1/4}}{[2j^{-2}(\sqrt{\lambda}\zeta_0)]^{1/4}}\frac{i}{\sqrt{2k}}\frac{e^{-iX}}{C+i\bar{D}/\lambda},\end{aligned} \tag{B.12}$$

where the irrelevant phase factor X reads

$$X\equiv\lambda\int_{y_i}^{y_2}\sqrt{-\hat{g}(y')}dy'+\frac{\pi}{4}+\phi\left(\frac{\lambda}{2}\zeta_0^2\right). \tag{B.13}$$

From Eq.(B.9) we conclude

$$\begin{aligned}C+i\frac{\bar{D}}{\lambda}&=\sqrt{C^2+\bar{D}^2/\lambda^2}e^{i\theta}\\&=(1+\mathcal{O}(1/\lambda^3))e^{i\theta},\end{aligned} \tag{B.14}$$

thus the coefficients α_1 and β_1 are given by,

$$\begin{aligned}\alpha_1&\simeq\frac{\lambda^{-1/4}}{[2j^2(\sqrt{\lambda}\zeta_0)]^{1/4}}\frac{e^{-i(X+\theta)}}{\sqrt{2k}},\\\beta_1&\simeq\frac{i\lambda^{-1/4}}{[2j^{-2}(\sqrt{\lambda}\zeta_0)]^{1/4}}\frac{e^{-i(X+\theta)}}{\sqrt{2k}}.\end{aligned} \tag{B.15}$$

Now we turn to match the approximate solution around y_1 and y_2 with the one around y_0. For the approximate solution around y_1 and y_2, when $\zeta\ll-|\zeta_0|$ (i.e., $y\ll y_1$), one has

$$\begin{aligned}\mu_k(y)\simeq\left(\frac{-1}{\lambda\hat{g}}\right)^{1/4}&\left\{\alpha_1(2j^{-2})^{1/4}\left(C\sin\mathfrak{D}-\frac{\bar{D}}{\lambda}\cos\mathfrak{D}\right)\right.\\&\left.+\beta_1(2j^2)^{1/4}\left(C\cos\mathfrak{D}+\frac{\bar{D}}{\lambda}\sin\mathfrak{D}\right)\right\}.\end{aligned} \tag{B.16}$$

Here

$$\begin{aligned}\mathfrak{D}&\equiv-\frac{\lambda}{2}\zeta\sqrt{\zeta^2-\zeta_0^2}-\frac{\lambda}{2}\zeta_0^2\ln\left(\frac{\sqrt{\zeta^2-\zeta_0^2}-\zeta}{\zeta_0}\right)\\&\quad+\frac{\pi}{4}+\phi\left(\frac{\lambda}{2}\zeta_0^2\right)\\&=-\lambda\int_{y_1}^{y}\sqrt{-\hat{g}}dy'+\frac{\pi}{4}+\phi\left(\frac{\lambda}{2}\zeta_0^2\right).\end{aligned} \tag{B.17}$$

Similar to the case when $y\to+\infty$ ($\zeta\gg|\xi_0|$), we assume that the turning points y_0 and y_1 are large spaced. Thus the coefficients $C=C(\lambda,\zeta)$ and $D=D(\lambda,\zeta)$ are given by

$$C(\lambda,\zeta)\simeq1-\frac{\mathscr{I}^2(\zeta)}{8\lambda^2}+\mathcal{O}\left(\lambda^{-3}\right),$$

$$\frac{D(\lambda,\zeta)}{\lambda} \simeq -\frac{\mathscr{I}(\zeta)}{2\lambda} + \mathcal{O}\left(\lambda^{-3}\right), \tag{B.18}$$

with $\mathscr{I}(\zeta)$ given by

$$\mathscr{I}(\zeta) = \int_{-\zeta_0}^{\zeta} \frac{\psi(v)}{\sqrt{v^2-\zeta_0^2}}. \tag{B.19}$$

Then let us turn to consider the approximate solution near y_0. When ξ is large enough (i.e., $y \gg y_0$), using the asymptotic expansions of Airy type functions given in Appendix A, we have

$$\mu_k(y) = \left(\frac{-1}{\lambda^{2/3}\hat{g}}\right)^{1/4} \left\{ \frac{\alpha_0}{\sqrt{\pi}} \left(A\cos\mathfrak{A} + \frac{\bar{B}}{\lambda}\sin\mathfrak{A} \right) + \frac{\beta_0}{\sqrt{\pi}} \left(-A\sin\mathfrak{A} + \frac{\bar{B}}{\lambda}\cos\mathfrak{A} \right) \right\}, \tag{B.20}$$

where $\bar{B} \equiv \sqrt{-\xi}B(\lambda,\xi)$ and

$$\mathfrak{A} \equiv \frac{2}{3}\lambda(-\xi)^{3/2} - \frac{\pi}{4} = \lambda\int_{y_0}^{y}\sqrt{-\hat{g}}dy' - \frac{\pi}{4}. \tag{B.21}$$

Up to the third-order approximation, one finds [16]

$$A(\lambda,\zeta) \simeq 1 - \frac{\mathscr{H}^2(\xi)}{8\lambda^2} + \mathcal{O}(\lambda^{-3}),$$
$$\frac{\bar{B}(\lambda,\zeta)}{\lambda} \simeq -\frac{\mathscr{H}(\xi)}{2\lambda} + \mathcal{O}\left(\lambda^{-3}\right), \tag{B.22}$$

with

$$\mathscr{H}(\xi) = \int_0^{\zeta} \frac{\psi(v)}{\sqrt{|v|}}dv. \tag{B.23}$$

Now combining Eqs.(B.16) and (B.20) we obtain

$$\alpha_0 \simeq \frac{\sqrt{\pi}}{\lambda^{1/12}} \left\{ \left[(2j^2)^{1/4}\beta_1\cos\mathfrak{B} + (2j^{-2})^{1/4}\alpha_1\sin\mathfrak{B}\right] + \frac{\mathscr{I}(\zeta)+\mathscr{H}(\xi)}{2\lambda}\left[(2j^{-2})^{1/4}\alpha_1\cos\mathfrak{B} - (2j^2)^{1/4}\beta_1\sin\mathfrak{B}\right] - \frac{1}{2}\left(\frac{\mathscr{I}(\zeta)+\mathscr{H}(\xi)}{2\lambda}\right)^2\left[(2j^2)^{1/4}\beta_1\cos\mathfrak{B} + (2j^{-2})^{1/4}\alpha_1\sin\mathfrak{B}\right] \right\},$$
$$\beta_0 \simeq \frac{\sqrt{\pi}}{\lambda^{1/12}} \left\{ \left[(2j^{-2})^{1/4}\alpha_1\cos\mathfrak{B} - (2j^2)^{1/4}\beta_1\sin\mathfrak{B}\right] - \frac{\mathscr{I}(\zeta)+\mathscr{H}(\xi)}{2\lambda}\left[(2j^2)^{1/4}\beta_1\cos\mathfrak{B} + (2j^{-2})^{1/4}\alpha_1\sin\mathfrak{B}\right] - \frac{1}{2}\left(\frac{\mathscr{I}(\zeta)+\mathscr{H}(\xi)}{2\lambda}\right)^2\left[(2j^{-2})^{1/4}\alpha_1\cos\mathfrak{B} - (2j^2)^{1/4}\beta_1\sin\mathfrak{B}\right] \right\}, \tag{B.24}$$

where

$$\mathfrak{B} \equiv \lambda\int_{y_0}^{y_1}\sqrt{-\hat{g}(y')}dy' + \phi\left(\frac{\lambda}{2}\zeta_0^2\right), \tag{B.25}$$

and

$$\mathscr{I}(\zeta)+\mathscr{H}(\xi) = \int_{-\zeta_0}^{\zeta(y)}\frac{\psi(v)}{\sqrt{v^2-\zeta_0^2}}dv + \int_0^{\xi(y)}\frac{\psi(v)}{\sqrt{-v}}dv. \tag{B.26}$$

It should be noted that, in order to match the high-order approximate solutions, one has to choose a point at which the two approximate solutions given, respectively, by Eq.(B.16) and Eq.(B.20), are matched. This is unlike the case in the first-order approximation, for which the solutions can be matched at any point between the turning points y_0 and y_1 (or $\mathrm{Re}(y_1)$ when y_1 is complex), provided that $\xi(y)$ and $\zeta^2(y)-\zeta_0^2$ both are large enough. While different matching points may lead to different results, one can employ the following way to reduce the errors. When we match the solution, we have used both the asymptotic expansions of Airy functions and parabolic cylinder functions, for example

$$\mathrm{Ai}(\lambda^{2/3}\xi) \simeq \frac{\lambda^{-1/6}}{\pi^{1/2}(-\xi)^{1/4}}\left[\cos\mathfrak{A} + \mathcal{O}(\xi^{-3/2})\right], \tag{B.27}$$

for $|\xi| \gg 1$ and

$$W(\tfrac{1}{2}\lambda\zeta_0^2, \sqrt{2\lambda}\zeta) \simeq \left(\frac{2j^2(\sqrt{\lambda}\zeta_0)}{\lambda(\zeta^2-\zeta_0^2)}\right)^{1/4}\left[\cos\mathfrak{D} + \mathcal{O}\left(\frac{1}{\zeta^2-\zeta_0^2}\right)\right] \tag{B.28}$$

for $\zeta^2 - \xi_0^2 \gg 1$. Thus, from the terms we have ignored in the above expansions, it seems that a good matching point should be around the range when

$$\frac{1}{|\xi|^{3/2}} \sim \frac{1}{\zeta^2-\zeta_0^2}. \tag{B.29}$$

In this paper, we shall always consider the matching when the above condition is satisfied.

2. Error analysis and comparison with numerical (exact) solution

In this subsection, we are going to study the above matched approximate solutions numerically in order to understand the matching process. We also provide the comparison between the approximate solutions and the numerical (exact) ones for several cases.

Let us first focus on the error control functions of the approximate solutions in different ranges. The error control functions $\mathscr{I}(\zeta)$ and $\mathscr{H}(\xi)$ are presented in Fig. 6. The left panel corresponds to the error control function $\mathscr{H}(\xi)$ around the turning point y_0, and the right panel corresponds to the error control function $\mathscr{I}(\zeta)$ around turning points y_1 and y_2. Although the error control function is not the exact error of the approximate solution, it can help us to understand the level of the errors qualitatively. Fig. 6 clearly shows that the error of the approximate solution peaks in the region where $y \to 0^+$. And in a de-Sitter background with $\nu = 3/2$, as we have shown in [16], the error control function $\mathscr{H}(\xi)$ goes to $1/9$ in the limit $y \to 0^+$. Another feature is that $\mathscr{H}(\xi)$ is not sensitive to the values of parameters b_1 and b_2, as well as ϵ_*. For the error control function $\mathscr{I}(\zeta)$, unlike $\mathscr{H}(\xi)$, Fig. 6 shows that $\mathscr{I}(\zeta)$ is sensitive to the value of ϵ_*, and for most cases it is extremely small compared to the value of $\mathscr{H}(\xi)$ as $y \to 0^+$. It is clear that $\mathscr{I}(\zeta)$ increases when the parameter ϵ_* increases.

The coefficients $A_1(\xi)$ and $B_0(\xi)$ associated with the Airy solutions are displayed in Fig. 7. The left panel corresponds to the evolution of $A_1(\xi)$ as a function of y, and the right panel corresponds to the evolution of $B_0(\xi)$. In this figure, the de-Sitter background is chosen. For the parabolic cylinder solutions, the corresponding coefficients $C_1(\zeta)$ and $D_0(\zeta)$ are presented in Fig. 8 as a function of y, where the left panel corresponds to $C_1(\zeta)$ and the right panel represents $D_0(\zeta)$. Similar to the case for the error control functions given in Fig. 6, now the coefficients $C_1(\zeta)$ and $D_0(\zeta)$ are extremely small and negligible, compared to the values of $A_1(\xi)$ and $B_0(\xi)$, respectively.

The comparison between the approximate solution and the numerical solution is displayed in Fig. 9. As we mentioned above, the errors of each order of approximation are different when $y \to 0^+$. It has been shown clearly in Fig. 9 that the third-order approximation does improve the precision of the first-order and second-order approximation in the limit $y \to 0^+$. Considering that the error of the third-order approximation is about 0.15%, however, the first-order, second-order, and the third-order approximation are almost identical to each other within this error when $y \sim y_1$ or $y \sim y_2$. This implies that, compared to the third-order approximations around the turning point y_0, the high-order approximations around the turning points y_1 and y_2 in general does not significantly improve the first-order approximation.

Appendix C: Asymptotical expansions of parabolic cylinder functions and Airy functions

The asymptotic expansion of parabolic cylinder functions $W(\frac{1}{2}\lambda\zeta_0^2, \pm\sqrt{2\lambda}\zeta)$ and $W(\frac{1}{2}\lambda\zeta_0^2, \pm\sqrt{2\lambda}\zeta)$ for $\zeta^2 - \zeta_0^2 \gg 1$ can be written as [27]

$$W(\tfrac{1}{2}\lambda\zeta_0^2, \sqrt{2\lambda}\zeta) = \left(\frac{2j^2(\sqrt{\lambda}\zeta_0)}{\lambda(\zeta^2-\zeta_0^2)}\right)^{1/4}\cos\mathfrak{D}, \tag{C.1}$$

$$W'(\tfrac{1}{2}\lambda\zeta_0^2, \sqrt{2\lambda}\zeta) = -\left(\frac{\lambda(\zeta^2-\zeta_0^2)}{2j^{-2}(\sqrt{\lambda}\zeta_0)}\right)^{1/4}\sin\mathfrak{D}, \tag{C.2}$$

$$W(\tfrac{1}{2}\lambda\zeta_0^2, -\sqrt{2\lambda}\zeta) = \left(\frac{2j^{-2}(\sqrt{\lambda}\zeta_0)}{\lambda(\zeta^2-\zeta_0^2)}\right)^{1/4}\sin\mathfrak{D}, \tag{C.3}$$

$$W'(\tfrac{1}{2}\lambda\zeta_0^2, -\sqrt{2\lambda}\zeta) = -\left(\frac{\lambda(\zeta^2-\zeta_0^2)}{2j^{2}(\sqrt{\lambda}\zeta_0)}\right)^{1/4}\cos\mathfrak{D}, \tag{C.4}$$

with

$$\mathfrak{D} \equiv \frac{1}{2}\lambda\zeta\sqrt{\zeta^2-\zeta_0^2} - \frac{1}{2}\lambda\zeta_0^2\ln\left(\frac{\zeta+\sqrt{\zeta^2-\zeta_0^2}}{\zeta_0}\right) + \frac{\pi}{4} + \phi\left(\frac{1}{2}\lambda\zeta_0^2\right). \tag{C.5}$$

Here

$$\phi(x) = \frac{x}{2} - \frac{x}{4}\ln x^2 + \frac{1}{2}\mathrm{ph}\Gamma\left(\frac{1}{2}+ix\right), \tag{C.6}$$

where the phase $\mathrm{ph}\Gamma(\frac{1}{2}+ix)$ is zero when $x = 0$ and is determined by continuity otherwise.

For Airy type functions $\mathrm{Ai}(x)$ and $\mathrm{Bi}(x)$ for large positive x (i.e., $x \gg 1$), the asymptotic expansions have the form [23]

$$\begin{aligned}
\mathrm{Ai}(x) &= \frac{1}{2\pi^{1/2}x^{1/4}}e^{-\frac{2}{3}x^{3/2}},\\
\mathrm{Bi}(x) &= \frac{1}{\pi^{1/2}x^{1/4}}e^{\frac{2}{3}x^{3/2}},\\
\mathrm{Ai}(-x) &= \frac{1}{\pi^{1/2}x^{1/4}}\cos\left(\frac{2}{3}x^{2/3}-\frac{\pi}{4}\right),\\
\mathrm{Bi}(-x) &= -\frac{1}{\pi^{1/2}x^{1/4}}\sin\left(\frac{2}{3}x^{2/3}-\frac{\pi}{4}\right).
\end{aligned} \tag{C.7}$$

[1] A.H. Guth, Inflationary universe: A possible solution to the horizon and flatness problems, Phys. Rev. D **23**, 347 (1981); A.A. Starobinsky, A new type of isotropic cosmological models without singularity, Phys. Lett. B **91**, 99 (1980); K. Sato, First-order phase transition of a vacuum and the expansion of the Universe, Mon. Not. R. Astron. Soc. **195**, 467 (1981); D. Baumann, TASI Lectures on Inflation, arXiv: 0907.5424.

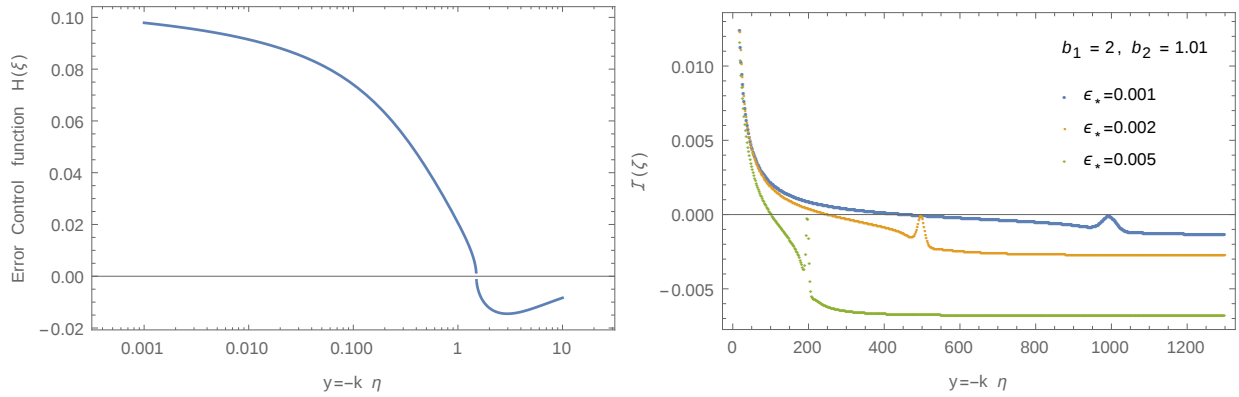

FIG. 6. Time evolution of the error control function. (a) Left panel: the error control function $\mathscr{H}(\xi)$ as a function of y in a de-Sitter background. (b) Right panel: the error control function $\mathscr{I}(\zeta)$ as a function of y in the de-Sitter background.

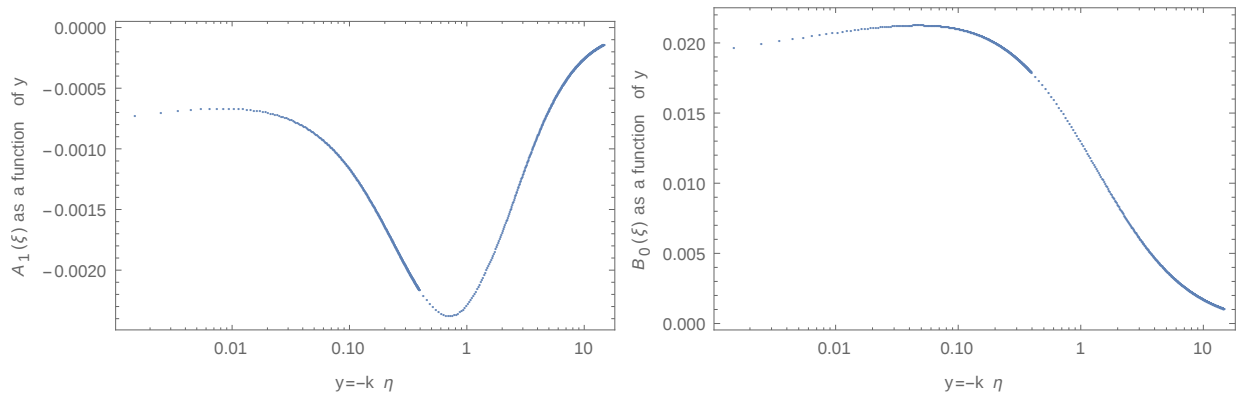

FIG. 7. Time evolution of the coefficients $A_1(\xi)$ and $B_0(\xi)$ associated with the Airy type solution around turning points y_0. (a) Left panel: $A_1(\xi)$ as a function of y in a de-Sitter background. (b) Right panel: $B_0(\xi)$ as a function of y in the de-Sitter background.

[2] E. Komatsu *et al.* (WMAP Collaboration), Seven-Year Wilkinson Microwave Anisotropy Probe (WMAP) Observations: Cosmological Interpretation, Astrophys. J. Suppl. Ser. **192**, 18 (2011); D. Larson *et al.* (WMAP Collaboration), Seven-Year Wilkinson Microwave Anisotropy Probe (WMAP) Observations: Power Spectra And Wmap - Derived Parameters, Astrophys. J. Suppl. Ser. **192**, 16 (2011).

[3] P. Ade *et al.* (PLANCK Collaboration), Planck 2013 results. XXII. Constraints on inflation, A&A 571, A22 (2014) [arXiv:1303.5082].

[4] P. A. R. Ade *et al.* (PLANCK Collaboration), Planck 2015 results. XX. Constraints on inflation, arXiv:1502.02114.

[5] R.H. Brandenberger, Inflationary Cosmology: Progress and Problems, arXiv:hep-th/9910410.

[6] J. Martin and R.H. Brandenberger, The Trans-Planckian Problem of Inflationary Cosmology, Phys. Rev. D **63**, 123501 (2001); J.C. Niemeyer and R. Parentani, Trans-Planckian dispersion and scale invariance of inflationary perturbations, *ibid.*, D **64**, 101301 (2001) (R); J. Martin and R.H. Brandenberger, Corley-Jacobson dispersion relation and trans-Planckian inflation, *ibid.*, D **65**, 103514 (2002); J. Martin and R.H. Brandenberger, Dependence of the spectra of fluctuations in inflationary cosmology on trans-Planckian physics, *ibid.*, D **68**, 063513 (2003); J. Martin and C. Ringeval, Superimposed oscillations in the WMAP data?, Phys. Rev. D **69**, 083515 (2004).

[7] R.H. Brandenberger and J. Martin, Trans-Planckian issues for inflationary cosmology, Class. Quantum. Grav. **30** (2013) 113001.

[8] A. Borde and A. Vilenkin, Eternal inflation and the initial singularity, Phys. Rev. Lett. **72**, 3305 (1994); A. Borde, A.H. Guth, and A. Vilenkin, Inflationary spacetimes are not past-complete, Phys. Rev. Lett. **90**, 151301 (2003).

[9] C.P. Burgess, J.M. Cline, F. Lemieux, and R. Holman, Are inflationary predictions sensitive to very high energy physics?, J. High Energy Phys. **02** (2003) 048; C.P. Burgess, J.M. Cline, and R. Holman, Effective Field Theories and Inflation, J. Cosmol. Astropart. Phys. **10** (2003) 004; N. Kaloper, M, Kleban, A.E. Lawrence, and S. Shenker, Signatures of Short Distance Physics in the Cosmic Microwave Background, Phys. Rev. D**66**, 123510 (2002).

[10] W.G. Unruh, Sonic analogue of black holes and the effects of high frequencies on black hole evaporation, Phys. Rev. D**51**, 2827 (1995); Hawking Spectrum and High Frequency Dispersion, S. Corley and T. Jacobson, *ibid.*, D**54**, 1568 (1996).

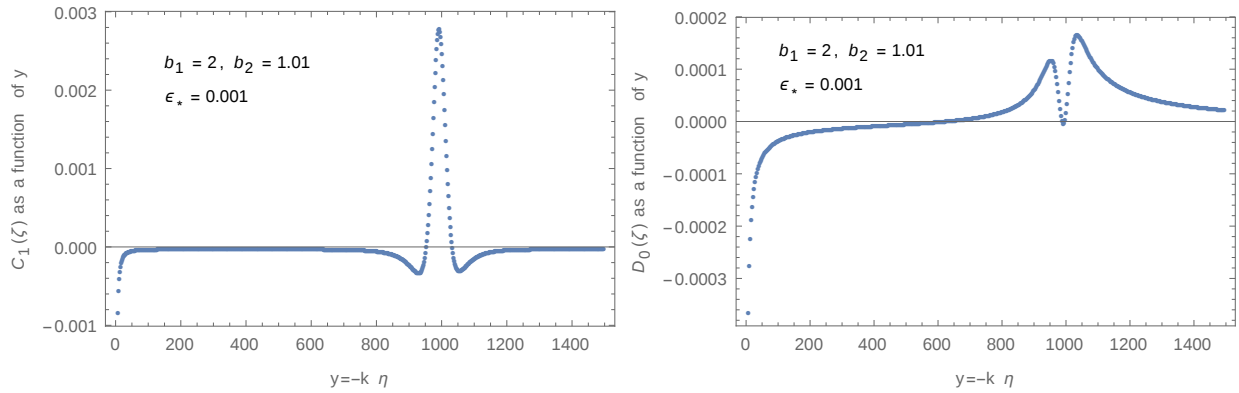

FIG. 8. Time evolution of the coefficients $C_1(\zeta)$ and $D_0(\zeta)$ associated with the parabolic cylinder function solutions around turning points y_1 and y_2. (a) Left panel: $C_1(\zeta)$ as a function of y in a de-Sitter background. (b) Right panel: $D_0(\zeta)$ as a function of y in the de-Sitter background.

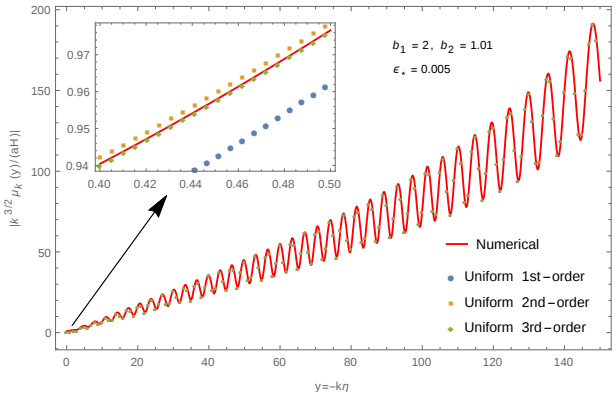

FIG. 9. Comparison of the analytical approximate solutions with different orders of approximations to the numerical (exact) solutions in a de Sitter background.

[11] S.E. Joras and G. Marozzi, Trans-Planckian physics from a nonlinear dispersion relation, Phys. Rev. D**79**, 023514 (2009); A. Ashoorioon, D. Chialva and U. Danielsson, Effects of nonlinear dispersion relations on non-Gaussianities, J. Cosmol. Astropart. Phys. **06**, 034 (2011).

[12] T. Takahashi and J. Soda, Chiral Primordial Gravitational Waves from a Lifshitz Point, Phys. Rev. Lett. **102**, 231301 (2009); K. Yamamoto, T. Kobayashi, and G. Nakamura, Breaking the scale invariance of the primordial power spectrum in Hořava-Lifshitz cosmology, Phys. Rev. D **80**, 063514 (2009); A. Wang and R. Maartens, Cosmological perturbations in Horava-Lifshitz theory without detailed balance, *ibid.*, D **81**, 024009 (2010); A. Wang, Vector and tensor perturbations in Horava-Lifshitz cosmology, *ibid.*, D **82**, 124063 (2010); Y.-Q. Huang and A. Wang, Non-Gaussianity of a single scalar field in general covariant Hořava-Lifshitz gravity, *ibid.*, D **86**, 103523 (2012); T. Zhu, F.-W. Shu, Q. Wu, and A. Wang, General covariant Horava-Lifshitz gravity without projectability condition and its applications to cosmology, *ibid.*, D **85**, 044053 (2012); E.G. M. Ferreira and R. Brandenberger, The Trans-Planckian Problem in the Healthy Extension of Hořava-Lifshitz Gravity, *ibid.*, D **86**, 86, 043514 (2012); T. Kobayashi, Y. Urakawa, and M. Yamaguchi, Cosmological perturbations in a healthy extension of Hořava gravity, J. Cosmol. Astropart. Phys. **04**, 025 (2010).

[13] Y.-Q. Huang, A. Wang, and Q. Wu, Inflation in general covariant theory of gravity, J. Cosmol. Astropart. Phys. **10**, 010 (2012); Inflation in general covariant Hořava-Lifshitz gravity without projectability, T. Zhu, Y.-Q. Huang, and A. Wang, J. High. Energy. Phys. **01**, 138 (2013).

[14] T. Zhu, A. Wang, G. Cleaver, K. Kirsten, and Q. Sheng, Inflationary cosmology with nonlinear dispersion relations, Phys. Rev. D **89**, 043507 (2014); Constructing analytical solutions of linear perturbations of inflation with modified dispersion relations, Int. J. Mod. Phys. A **29**, 1450142 (2014).

[15] S. Habib, K. Heitmann, G. Jungman, and C. Molina-Paris, The Inflationary Perturbation Spectrum, Phys. Rev. Lett. **89**, 281301 (2002); S. Habib, A. Heinen, K. Heitmann, G. Jungman, and C. Molina-Paris, Characterizing inflationary perturbations: The uniform approximation, Phys. Rev. D **70**, 083507 (2004); Inflationary perturbations and precision cosmology, S. Habib, A.Heinen, K. Heitmann, and G. Jungman, Phys. Rev. D **71**, 043518 (2005).

[16] T. Zhu, A. Wang, G. Cleaver, K. Kirsten, and Q. Sheng, Gravitational quantum effects on power spectra and spectral indices with higher-order corrections, Phys. Rev. D **90**, 063503 (2014).

[17] T. Zhu, A. Wang, G. Cleaver, K. Kirsten, and Q. Sheng, Power spectra and spectral indices of k-inflation: high-order corrections, Phys. Rev. D **90**, 103517 (2014).

[18] T. Zhu, A. Wang, G. Cleaver, K. Kirsten, Q. Sheng, and Q. Wu, Detecting quantum gravitational effects of loop quantum cosmology in the early universe?, Astrophys. J. Lett. **807**, L17 (2015); Scalar and tensor perturbations in loop quantum cosmology: High-order corrections, J. Cosmol. Astropart. Phys. 10, 052 (2015); T. Zhu, A. Wang, K. Kirsten, G. Cleaver, Q. Sheng, and Q. Wu, Inflationary spectra with inverse-volume corrections in loop quantum cosmology and their observational constraints from Planck 2015 data, J. Cosmol. Astropart. Phys. 03,

046 (2016).

[19] K. N. Abazajian, K. Arnold, J. Austermann, B. A. Benson *et al.*, Inflation physics from the cosmic microwave background and large scale structure, Astropart. Phys. **63**, 55 (2015).

[20] A.A. Starobinsky, Robustness of the inflationary perturbation spectrum to trans-Planckian physics, JETP Lett. **73**, 371 (2001).

[21] M. Lemoine, M. Lubo, J. Martin, and J.-P. Uzan, Stress-energy tensor for trans-Planckian cosmology, Phys. Rev. D **65**, 023510 (2001); R. H. Brandenberger and J. Martin, Back-reaction and the trans-Planckian problem of inflation reexamined, Phys. Rev. D **71**, 023504 (2005).

[22] B. R. Greene, K. Schalm, G. Shiu, and J. P. van der Schaar, Decoupling in an expanding universe: backreaction barely constrains short distance effects in the CMB, J. Cosmol. Astropart. Phys. 02 (2005) 001.

[23] F.W.J. Olver, Asymptotics and Special functions, (AKP Classics, Wellesley, MA 1997).

[24] F.W.J. Olver, Second-order Linear Differential Equations with two turning points, Phil. Trans. R. Soc. A **278**, 137 (1975).

[25] P. Hořava, Quantum gravity at a Lifshitz point, Phys. Rev. D **79**, 084008 (2009).

[26] D. Blas, O. Pujolas, and S. Sibiryakov, Consistent Extension of Hořava Gravity, Phys. Rev. Lett. **104**, 181302 (2010); Comment on "Strong coupling in extended Hořava-Lifshitz gravity", Phys. Lett. B **688**, 350 (2010); Models of non-relativistic quantum gravity: the good, the bad and the healthy, J. High Energy Phys., **1104**, 018 (2011).

[27] A. Gil, J. Segura, and N.M. Temme, Fast and accurate computation of the Weber parabolic cylinder function $W(a, x)$, IMA Journal of Numerical Analysis **31**, 1194 (2011).